PEOPLE'S DEMOCRATIC REPUBLIC OF ALGERIA

MINISTRY OF HIGHER EDUCATION AND SCIENTIFIC RESEARCH

MOHAMED BOUDIAF UNIVERSITY - M'SILA

FACULTY OF TECHNOLOGY
DEPARTMENT OF ELECTRICAL ENGINEERING
N°: ER-07

DOMAIN: SCIENCE AND TECHNOLOGY
SECTION: RENEWABLE ENERGIES
SPECIALITY: RENEWABLE ENERGIES IN ELECTROTECHNICS

Thesis presented for obtaining

Academic Master's degree

By:

YAHIAOUI Douaa

Entitled:

Charge Controller Design of a Stand-alone Photovoltaic System with Fuzzy logic MPPT Technique

Presented before the jury composed of:

RAHALI Hilal	University of M'sila	President
MAYOUF Messaoud	University of M'sila	Supervisor
CHERIF Bilal Djamel Eddine	University of M'sila	Examiner

Academic year: 2022/ 2023

Thank

بِسْمِ اللهِ الرَّحْمٰنِ الرَّحِيْمِ

Above all, I thank الله عز وجل for giving me strength and courage.

Next, I would like to sincerely thank Dr. Mayouf Messaoud my supervisor who provided enormous efforts, through his Information, his advice and his encouragement. I would also like to thank all the members of the jury for having accepted to examine this work, and to thank all the professors in the electrical engineering department.

My sincere thanks to my dear mother and my dear father, for their unconditional support and precious help throughout my studies. Their presence and constant support deserve my deepest gratitude.

My warm thanks to all near and far who contributed to reach this thesis.

Dedication

To my parents Abdelkader and Hanane, who have always believed in me, provided unwavering support, and instilled in me the value of education. This thesis is dedicated to you for your endless love and encouragement. To my grandmother Ftaima, my brothers Abdelhak and Abdelbaki, my sisters Hana, Safa, Maroua, Raja. to my fiance Farid, to my uncles and aunts each in his name, to my friends and classmates. To all my relatives and my acquaintances, to all those who have studied me, each in their own name and position, to the memory of my teacher Radhia, whose passion for knowledge continues to inspire me. To the souls of my grandfathers and my grandmother.

To all dear to my heart.

Douaa

Summary

List of abbreviations

G	Solar irradiance, W/m²
I_{pvM}	Instantaneous current of maximum point MPP, A
I_{ph}	Photon current of PV cell, A
I_{pv}	PV cell output current, A
I_d	Diode current, A
I_s	Diode saturation current, A
T_c	PV cell temperature, K
V_d	Diode voltage, V
V_{pvM}	MPP maximum point instantaneous voltage, V
V_{oc}	Open circuit voltage, V
V_{pv}	Voltage across PV cell, V
V_t	Voltage across p–n junction, V
αT	Temperature coefficient on PV current
βT	Temperature coefficient on PV voltage
λT	Irradiance coefficient on PV power
A_n	Diode ideality factor
IMS	PV current at point MPP under STS conditions, A
I_{ph}	PV photon current under STC conditions, A
ISCS	PV short-circuit current at the STC, A
PMPP	PV power at MPP point under STC conditions, W
R_s	Series resistance, Ω
R_{sh}	Parallel resistance, Ω
VMS	PV voltage at MPP point under STC conditions, V
V_{ocs}	The open circuit PV voltage under STC conditions, V
FF	Fill factor
Pm	The maximum output power

List of figures

GENERAL INTRODUCTION

General introduction

Renewable energy is increasingly becoming a promising solution due to the rising costs of conventional energy sources and the limited availability of their resources. It offers several advantages, including abundance, absence of pollution, and availability in varying quantities worldwide.

Renewable energy sources encompass solar power, wind energy, geothermal energy, hydropower, tidal energy, and biomass. These sources operate with minimal or no waste generation and pollutants, positioning them as the energy of the future. Different technological sectors exist within renewable energy, depending on the specific energy source harnessed and the resulting useful energy obtained.

The primary focus of this thesis revolves around the examination of photovoltaic energy. Nonetheless, there are significant challenges associated with this energy source, namely the high cost of generators and the relatively low energy efficiency. In order to address these issues, it is essential to prioritize the control and optimization of photovoltaic systems.

Problematic

How can we control our battery and optimize our photovoltaic system in the same time with single converter?

Purpose of work

This work is based on the study of a stand-alone photovoltaic system, the control of the battery charging process and the optimization with fuzzy logic technique, to achieve this objective, we have divided our dissertation into three chapters in addition to the general introduction and conclusion.

Thesis structure

The first chapter presents a generality on the photovoltaic system, the operating principle, and their advantages and disadvantages.

Then, we will move on to the second chapter devoted to the modeling of the photovoltaic panel, we will show the photovoltaic system simulation results and analyze the following two effects: temperature and irradiance.

In the last chapter, we will present an MPPT command based on a fuzzy controller, many simulations and analyzes are presented, then we will show the simulation results of a PV system with the Fuzzy-MPPT controller.

Chapter 1

State of the art on photovoltaic systems

1.1 Introduction

Various renewable energy sources, such as the sun, water, and wind, play a significant role in the generation of sustainable energy. Solar energy, derived from the sun, is extensively utilized for electricity production and heat generation. Within the realm of solar energy, photovoltaic energy stands out as a relatively new form. Credit for the discovery of the photovoltaic effect, the ability to convert light energy into electricity, is attributed to the French physicist Alexandre Becquerel in 1839. His breakthrough unlocked the potential for harnessing solar energy as a viable source of electricity.

This chapter will provide a concise overview of the PV generator, including its composition, operational principle, various PV cell technologies, and the diverse electrical configurations employed in the domain of photovoltaic energy conversion. The aim is to develop a comprehensive understanding of photovoltaic systems.

1.2 Renewable energies

Renewable energies encompass natural resources such as the sun and wind, which possess the advantage of being perpetually replenished and do not deplete over time. These energy sources are continuously renewed at a rate that exceeds their consumption, making them sustainable for the long term. Moreover, renewable energies are accessible in most regions across the globe. Among these renewable energies are: Wind energy Solar energy. Geothermal energy, hydropower, tidal energy, biomass, biofuels.

1.3 Solar energy source

The sun serves as an abundant and nearly limitless energy source, radiating vast amounts of energy towards the Earth's surface. In fact, the amount of solar irradiance received annually is estimated to be around 8400 times the total global energy consumption. This equates to an average instantaneous power of 1 kilowatt peak per square meter (KWp/m^2), encompassing the full spectrum of energy from ultraviolet to infrared wavelengths. The deserts of our planet receive in 6 hours more energy from the sun than consumes humanity in a year. Solar energy is produced and used in several processes [1]. Solar energy offers a self-contained and environmentally-friendly source of power, devoid of any pollution., reliable, quiet, long-term, maintenance-free, and year-round continuous and unlimited operation at moderate costs [2].

1.3.1 Main types of solar energy

1.3.1.1 Solar thermal energy (for heating)

Solar thermal energy, also referred to as solar thermal power or thermoelectricity, is a renewable energy source that harnesses the sun's heat to generate large-scale, clean electricity.

Similar to photovoltaic energy that converts sunlight into electricity using solar cells, solar thermal technology utilizes the sun's heat to warm liquids, produce steam, and generate electricity through a conventional thermal process.

1.3.1.2 Concentrated solar power (for electricity)

The concentrated solar power is one of the most popular types of solar energy, it uses mirrors to reflect and concentrate sunlight onto a receiver. The intense sunlight is focused to heat a high-temperature fluid within the receiver. Spain holds the top position globally when it comes to utilizing Concentrated Solar Thermal (CST) technology for electricity generation.

1.3.1.3 Passive energy

Solar photovoltaic and solar thermal energy use different technologies to capture and process solar energy. This is called active solar energy. However, solar energy can also be used passively, Passive solar technologies utilize sunlight to generate usable heat and facilitate air movement, enabling the heating and cooling of living spaces without the reliance on mechanical devices or electrical systems.

1.3.1.4 Photovoltaic solar energy (electricity)

Photovoltaic solar power provides light that is converted into electricity through photovoltaic solar panels. These photovoltaic solar panels are made up of groups of cells or solar cells that convert light (photons) into electrical energy (electrons) [3]. Photovoltaic solar energy involves harnessing electricity directly from sunlight. This is accomplished by installing solar panels composed of silicon cells that convert solar irradiance into electrical energy by utilizing light and heat. These panels can be installed on various scales, ranging from individual buildings and homes to larger-scale installations.

1.4 Photovoltaic conversion principle

Photovoltaic conversion, which is widely used today, can be simply defined as the transformation of photon energy into electrical energy through the process of absorption light by matter. When a photon is absorbed by the material, through collision with an electron, a portion of its energy is transferred, effectively dislodging the electron from its original position within the matter. This electron, previously in a stable state at a lower energy level, transitions to a higher energy level, inducing an electrical imbalance within the material. As a consequence, an electron-hole pair is created, each possessing an equivalent electrical energy. [4].

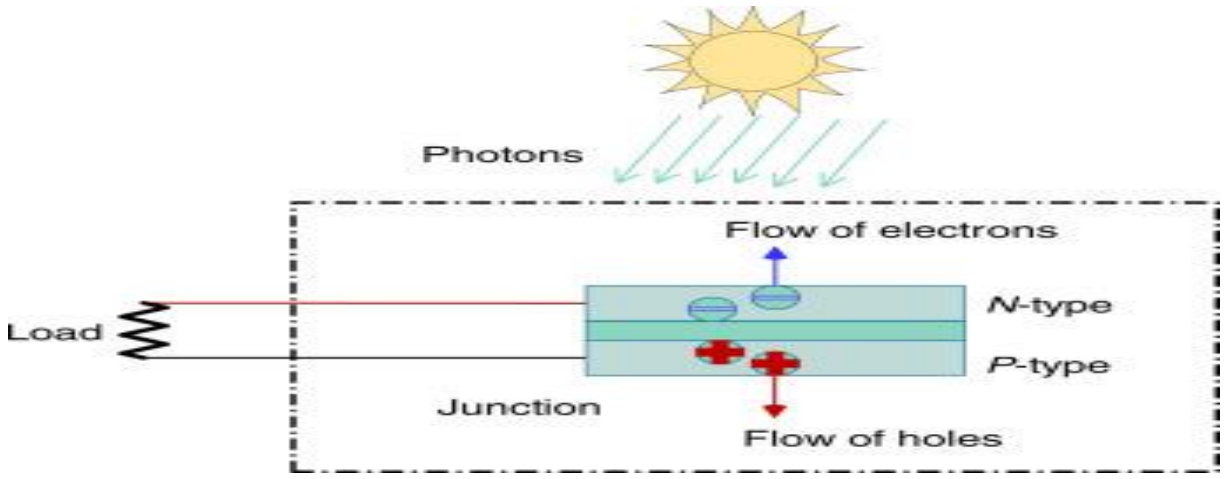

Figure 1-1: Principle of photovoltaic effect for photon to electrical energy conversion. [5]

When a photon is absorbed by a material, the resulting energy manifests electrically through the generation of an electron-hole pair. This process causes a redistribution of charges, leading to a variation in electrical potential. This phenomenon is known as the photovoltaic effect. The fact of having associated two types of materials to create a junction makes it possible to be able to recover the charges before they have recombined in the material which then becomes neutral again. The presence of the PN junction thus makes it possible to maintain a current flow to its terminals. The number of photons per unit wavelength is a data to know for photovoltaic applications to estimate the total energy available. The wavelength corresponding to the maximum of photons is of the order of 650-670nm.

1.5 The photovoltaic effect

The photovoltaic effect is a mechanism that transforms light, specifically photons, into electrical energy. Solar cells, also known as photovoltaic (PV) cells, are electronic devices that directly convert sunlight into electricity by leveraging the photovoltaic effect. A photovoltaic system consists of an array of solar modules, composed of multiple solar cells, which collectively generate electrical power.

The photovoltaic effect occurs in solar cells. These solar cells are composed of two different types of semiconductors - a p-type and an n-type - that are joined together to create a p-n junction. To read the background on what these semiconductors are and what the junction is. By joining these two types of semiconductors, an electric field is formed in the region of the junction as electrons move to the positive p-side and holes move to the negative n-side. This field causes negatively charged particles to move in one direction and positively charged particles in the other direction. [6]

Light consists of photons, which are essentially small beams of electromagnetic irradiance or energy. Photovoltaic cells, which are the building blocks of solar panels, have the capability to absorb these photons. When light with the appropriate wavelength illuminates these cells, the energy of the photons is transferred to an atom within the semiconductor material at the p-n junction. Specifically, the energy is transferred to the electrons present in the material. As a consequence of this process, the electrons undergo a transition to a higher energy state known as the conduction band. This transition results in the creation of an empty space, known as a "hole," in the valence band where the electron was initially located. The movement of the electron, propelled by the acquired energy, generates a pair of charge carriers comprising both the electron and the hole.

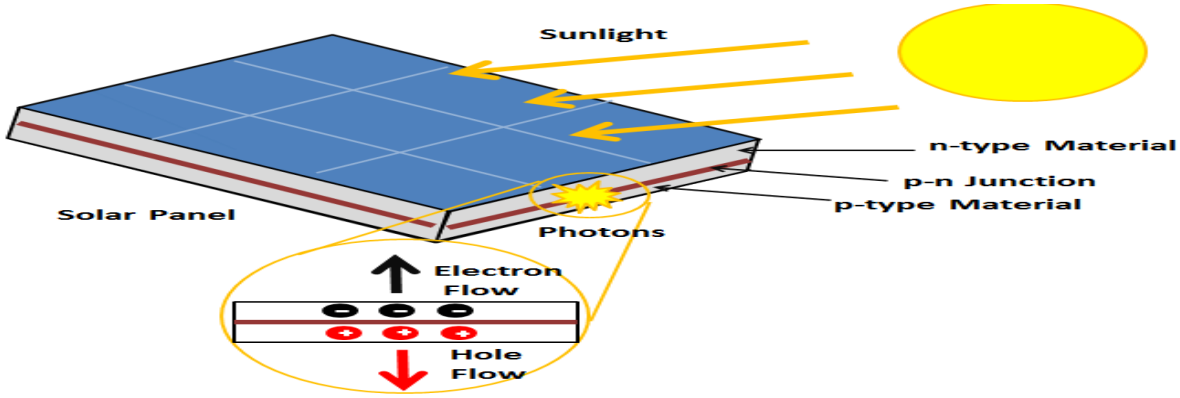

Figure 1-2: The photovoltaic effect. [6]

When unexcited, electrons hold the semiconductor material together by forming bonds with surrounding atoms and are therefore unable to move. However, in their excited state in the conduction band, these electrons are free to move through the material. Since the electric field exists due to the p-n junction, the electrons and holes move in the opposite direction as expected. Instead of being attracted towards p, the released electron tends to move towards n. This movement of electrons creates an electric current in the cell.[7] As the electron moves, a "hole" remains. The hole can also move, but in the opposite direction to the p-side. This process creates an electric current in the cell. A diagram of this process can be seen in figure (1-2).

1.5.1 Different types of photovoltaic systems

1.5.1.1 On-grid system

The on-grid system is the prevalent choice, as it connects directly to the power grid and does not require any batteries. This system enables owners to draw power from both the solar system

and the grid. When the solar panels or system generate surplus energy beyond the current consumption, the excess power is fed back into the grid, thus providing credit or compensation from the grid power company.

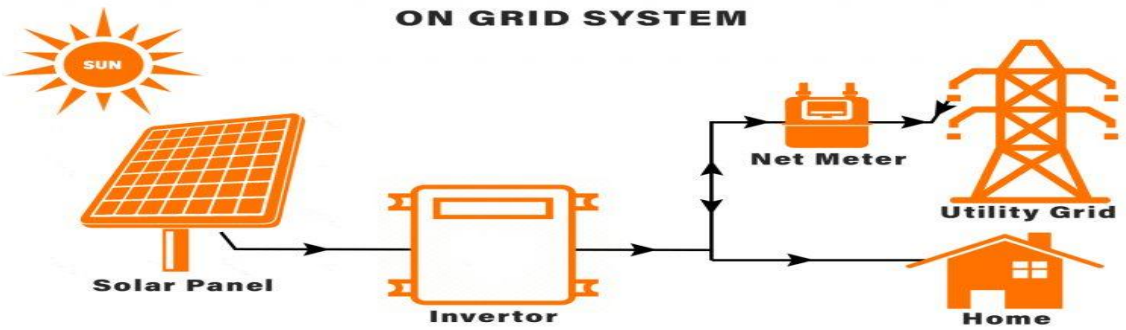

Figure 1-3: On-grid system [8].

1.5.1.2 Off-grid system (Stand-alone)

An off-grid solar power system operates independently without any connection to the grid, necessitating the use of battery storage. This type of system is capable of generating electricity in remote locations where grid access is limited or unavailable, making it desirable for those seeking self-sufficiency. While similar to an on-grid system in many aspects, an off-grid system incorporates additional components to support its autonomous functionality.

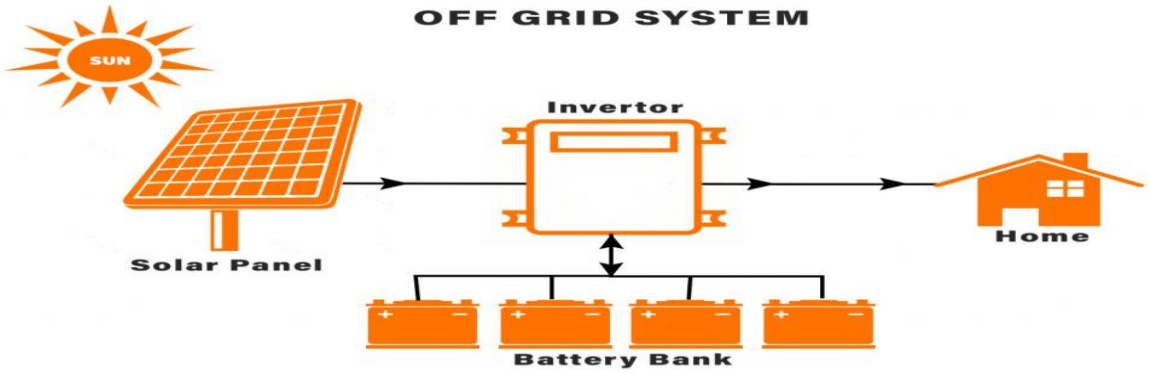

Figure 1-4: Off-grid system [8].

1.5.1.3 Hybrid system

Hybrid systems integrate the principles of both off-grid and on-grid systems, creating a combined solution that combines a grid-connected solar system with battery storage. These systems employ batteries to store excess energy, which can be utilized during periods of high energy demand or when solar production is limited due to insufficient sunlight. In instances when the stored energy is depleted, the grid serves as a backup power source, enabling users to utilize both power sources. The primary objective of hybrid systems is to assist in minimizing peak energy consumption during daylight hours.

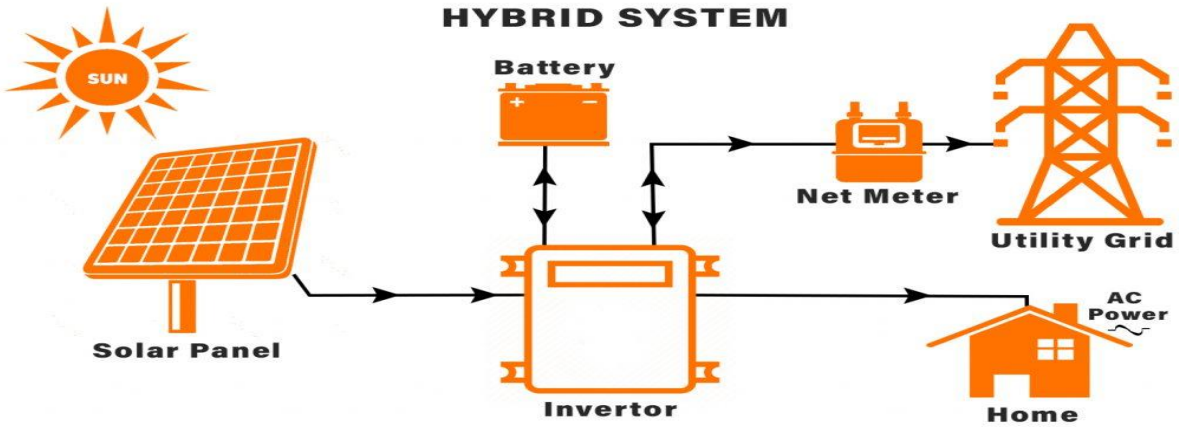

Figure 1-5: Hybrid system. [8]

1.6 Solar irradiance

Solar irradiance, commonly known as solar energy or simply sunlight, encompasses the electromagnetic irradiance emitted by the sun. This radiant energy can be harnessed and transformed into practical forms of energy, including heat and electricity, using diverse technologies. Nevertheless, the feasibility and cost-effectiveness of implementing these technologies in a specific location are contingent upon the accessibility of solar energy resources.

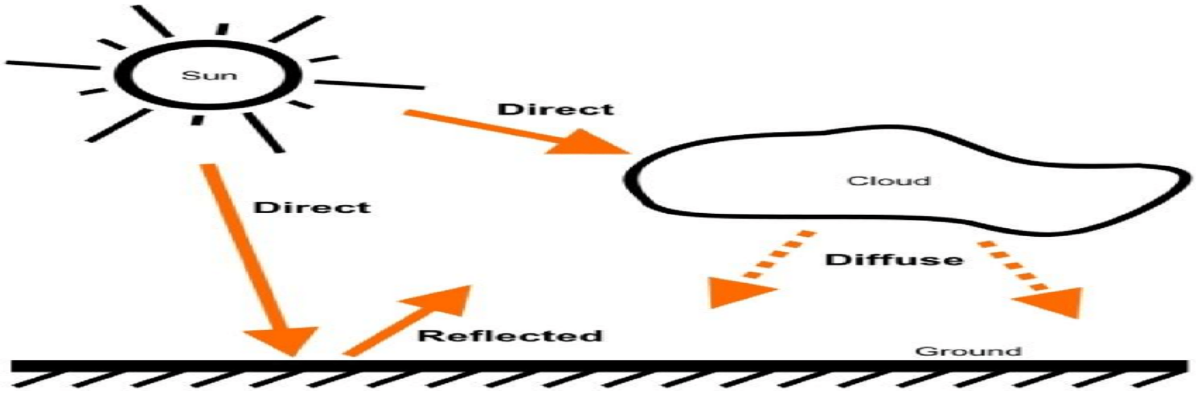

Figure 1-6: Types of solar irradiance received on the ground [9].

In fact, four types of irradiances have been listed in the literature:

1.6.1 Direct beam solar irradiance

Direct irradiance on the horizontal plane, is the difference between global irradiance and diffuse irradiance.

1.6.2 Diffuse solar irradiance

This is due to the absorption and scattering of part of the irradiance global solar irradiance by the atmosphere and its reflection by clouds and aerosols.

1.6.3 Reflected irradiance

The term "albedo" refers to the irradiance that is reflected by the Earth's surface or objects present on the surface. In cases where the ground exhibits high reflectivity, such as water bodies or snow-covered areas, the albedo effect becomes notably significant.

1.6.4 Global irradiance

Global irradiance is subdivided into direct, diffuse and ground-reflected irradiance).

The intensity of solar irradiance received on any plane at any given time is called irradiance or illumination (usually denoted by the letter G), it is expressed in watts per square meter (W/m^2) [10]. The value of irradiance received by the surface of the photovoltaic module varies depending on the position of the latter. Solar irradiance reaches its maximum intensity when the plane of the photovoltaic module is perpendicular to the rays.

1.7 The PV panel or module

The photovoltaic module, comprised of interconnected solar cells, stands as a pivotal component within any PV installation. These modules are interconnected to form fields so that different levels of energy requirements can be met. More and more powerful modules are available on the market, in particular for network connection, but there is still a limit related to weight and handling [11].

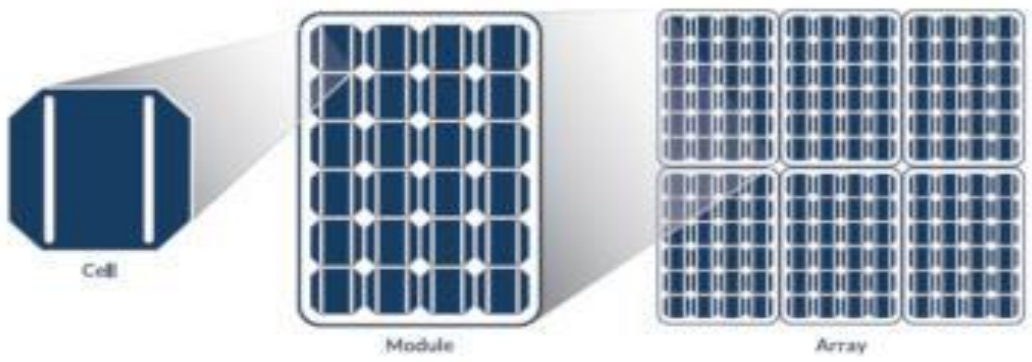

Figure 1-7: Solar Cell, Module, and Array.[12]

The curve in the figure (1-8) shows the non-linear characteristics of the photovoltaic module, which is particularly dependent on sunlight and temperature conditions. However, several important electrical quantities describe the operation of the photovoltaic module.

- Maximum current (Isc). This happens when the module terminals are shorted together. It is called the short circuit current (Isc) and depends a lot on the level of irradiance.
- No-load voltage (Voc) for zero current. This voltage is called the open-circuit voltage.
- Optimal operating point PPM (maximum module power).

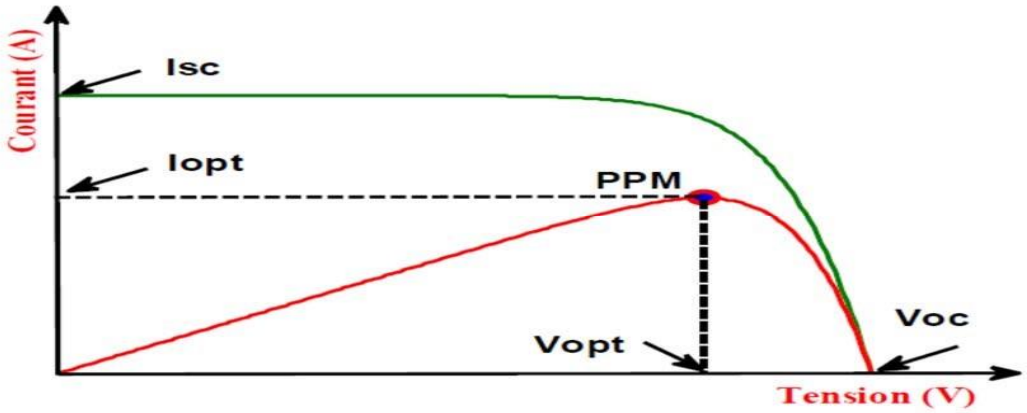

Figure 1-8: Electrical characteristics of the photovoltaic module. [13]

1.8 The PV cell

A photovoltaic solar cell is an electronic semiconductor device that, when exposed to light, produces a DC voltage.

1.8.1 Principle of operation of the photovoltaic cell

The functioning of the photovoltaic cell is based on the collision of photosynthetic molecules (photons) with a semiconductor element such as silicon, which separates the electrons of their atoms. Thus, the extra electrons are scattered randomly.

By incorporating two types of silicon, the control over electron movement is established. The first side is doped with phosphorus atoms, which possess an excess of electrons compared to silicon, resulting in a negatively charged region known as the N-type region.

On the other hand, it is anesthetized by boron atoms which contain a smaller number of silicon electrons, so that they become positively charged due to a lack of electrons called the narcotic P region. This dual face becomes a bit like a battery called (pn junction).

By adding metal contacts on the n and p areas, a diode is obtained. When the junction is illuminated, the photons of energy equal to or greater than the width of the forbidden band impart their energy to the atoms, each of which passes an electron from the valence band into the conduction band and also leaves a hole capable of move, thus generating an electron-hole pair. When a voltage is applied across the terminals of the cell, the electrons in the N region migrate towards the holes in the P region through the external circuit, creating a potential difference [14].

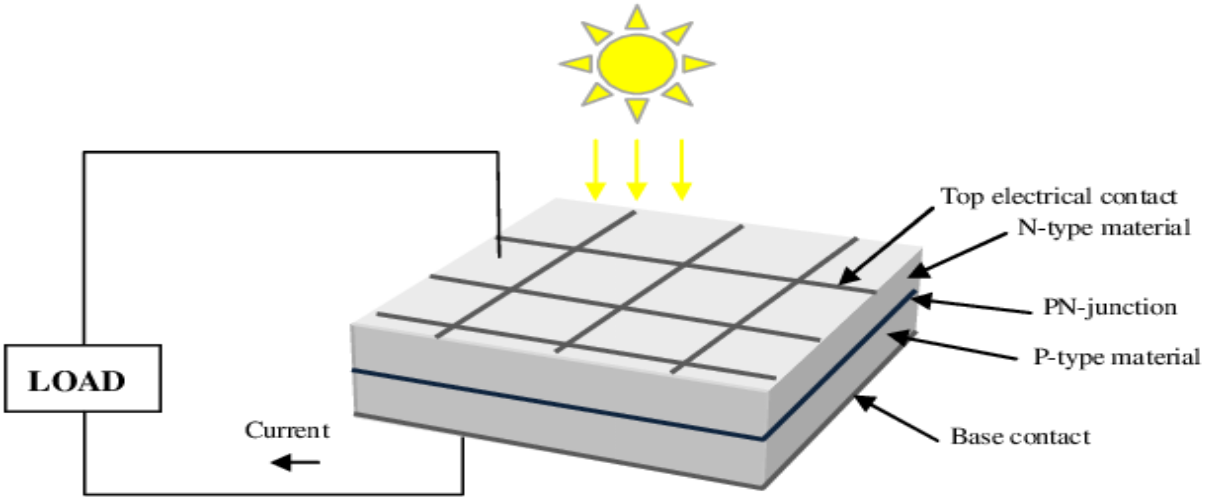

Figure 1-9: Basic solar cell construction [15].

1.8.2 Association of photovoltaic cells

The photovoltaic cell generates 2.3 (Wp) under a potential difference of approximately 0.5 Volts. This low power is not enough for most domestic or industrial photovoltaic applications. To obtain high voltage and power, several photovoltaic cells must be connected together, in series and/or parallel.

1.8.2.1 Serial association

When Ns PV cells are connected in series, the voltages of these cells add up and the current generated is the same across the entire branch. Result IV characteristic of association in figure (1-10) is obtained by multiplying each point and for the same current, the individual voltage Vi by Ns. We also note that the optimal impedance of the association will be Ns times greater than the impedance of the base cell.

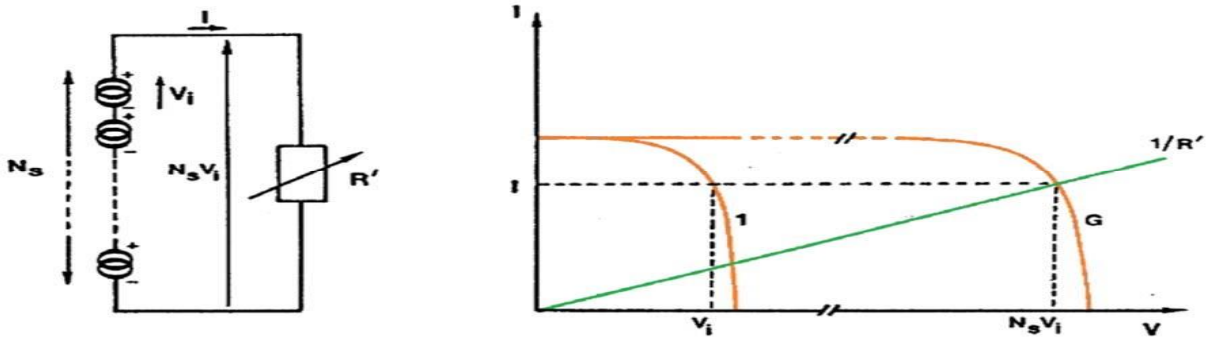

Figure 1-10: Association of Ns cells in series. [13]

The current generated by Ns PV cells in series is the same throughout the branch and is limited by the current of the weakest cell. Care must be taken to connect only cells of the same current density in series. This is why during the manufacturing process all cells are tested and sorted according to their performance. The series resistances add up and increasing the series resistance will cause power loss. Therefore, it is necessary to pay attention to the link resistance of the cells, in a series link. The form factor of a module in general cannot be better than the form factor of its constituent cells. For the current, it approaches the worst cell. Parallel resistors are also added.

1.8.2.2 The parallel association

That is the voltage of each cell should be identical, the current is added. The new curve in figure (1-11) is obtained by adding points one by one and for each voltage value, the base current of the cell in Np. The optimal impedance of the association will be Np times less than the impedance of an individual cell.

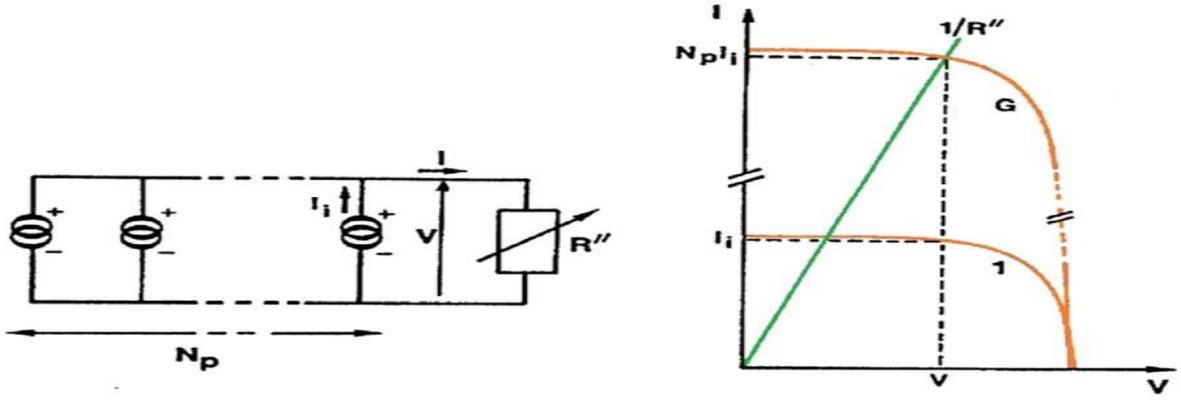

Figure 1-11: Association of Np cells in parallel. [13]

Silicon PV solar cells are made from sliced high purity silicon ingots or sliced ingots. The manufacturing process creates a charge separation junction, deposition of passive layers and anti-reflective coating, and the addition of metal contacts. The module is then covered with transparent glass and weather-resistant materials and mounted on the surrounding frame.

Two main families of PV materials can be distinguished:

- Crystalline solids.
- Solid thin layers or thin film.

1.8.3 The different types of solar cells (photovoltaic cells)

There are different types of solar cells or photovoltaic cells. Each type of cell is characterized by has a yield and a cost which are specific to it However, whatever the type, the efficiency remains quite low: between 8 and 3% of the energy that the cells receive [14].

Currently, there are three main types of cells:

a. Monocrystalline cells

They have the best yield (from 12 to 18% or even up to 24% in the laboratory) However, they are too expensive due to their complex manufacture.

b. Polycrystalline cells

Their design is easier and their manufacturing cost is lower. However, their yield is lower (from 11% to 15% or even up to 19.8 in the laboratory).

c. Amorphous cells

They have a low yield (from 5% to 8% or even up to 13% in the laboratory), but do not require only very small thicknesses of silicon and have a low cost. They are commonly used in small consumer products such as calculators, sunglasses or even watches. The advantage of this last type is that it works with a low solar irradiance (even on a cloudy day or inside a building).

Figure 1-12: Monocrystalline, polycrystalline and amorphous cells.[16]

1.9 The PV field

The photovoltaic array is composed of interconnected photovoltaic modules arranged in series and/or parallel configurations to generate the desired power output. These modules are mounted

on a metal frame, which provides structural support and allows for the specific tilt angle of the PV array [11].

1.10 Advantages and disadvantages of photovoltaic energy

1.10.1 Advantages

- The sun is the hope of some remote areas about electricity.
- Their systems can be installed above surfaces as there is no space for their installation.
- Photovoltaic technology has qualities from an ecological point of view because the finished product, is non-polluting, silent and does not disturb the environment.
- Free consumption upon installation of the system.
- The solar panel has a long service life.
- The modular nature of the photovoltaic panels allows for simple and adaptable to various energy needs. Systems can be sized for power applications ranging from MilliWatt to MegaWatt [17].

1.10.2 Disadvantages

- The cost of building electrical systems is very high.
- Dependent on weather conditions.
- the actual efficiency of a photovoltaic module is around 10 to 15%.
- The storage of electrical energy still poses many problems.
- When the storage of electrical energy in chemical form (battery) is necessary, the cost of the generator is increased.

1.11 Conclusion

This first chapter is an introduction to our work. We have presented some generalities on photovoltaic systems, principle of converting solar energy into electrical energy by photovoltaic cell, as well as the different system configurations photovoltaic we presented the main characteristics and technological components of the photovoltaic system, which we studied the operating principle of the photovoltaic cell and we presented their types of cells (monocrystalline, polycrystalline, amorphous), finally we have listed the advantages and disadvantages of PV systems in general.

Chapter 2

Modeling and simulation of photovoltaic panel

2.1 Introduction

The photovoltaic module serves as a medium for converting light into electricity. To accurately model this device, meteorological data such as irradiance and temperature are essential input variables. The output of the module can be in the form of current, voltage, power, or other relevant parameters. The I(V) or P(V) characteristics of the module are specifically designed to accommodate these variables. Any alteration in the input values results in an immediate impact on the output. Therefore, selecting the appropriate PV module is crucial to ensure optimal performance.

The most used models are:

1. Ideal single diode model

2. single diode model

3. two-diode model

In this chapter, we will review mathematical models of photovoltaic cells and panels, and then we will present the implementation of these models using MATLAB/SUMILINK. The results of the simulations performed will be presented and then interpreted.

2.2 Electrical characteristics of a photovoltaic cell

Figure (2-1) presents the equivalent diagram of a photovoltaic cell under solar irradiance. It corresponds to a current generator (I_{Ph}) connected in parallel with a diode. Two parasitic resistances are introduced in this scheme. These resistors have some effect on the *I = f(V)* characteristic of the cell:

- The series resistance (R_s) is the internal resistance of the cell; it depends mainly the resistance of the semiconductor used, the contact resistance of the collector grid and the resistivity of these grids;
- Shunt resistance (R_{sh}) due to leakage current at the junction; it depends on how it was done.

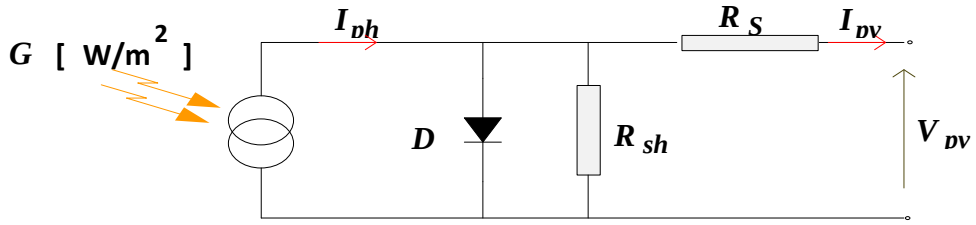

Figure 2-1 Equivalent electrical scheme of a photovoltaic cell. [18]

A static model of a photovoltaic cell can be described by the following electrical equation:

$$I_{pv} = I_{Ph} - I_s\left(exp\frac{(V_{pv} + I_{pv} * R_s)}{A_n * k * T_c} - 1\right) - \frac{V_{pv} + I_{pv} * R_s}{R_{sh}} \qquad (2.1)$$

Where:

I_s is diode saturation current,

I_{Ph} is photo-current,

Vt thermal voltage (temperature function),

R_s and R_{sh} are the series and shunt resistances respectively.

2.3 Parameters of a photovoltaic cell

The parameters of the photovoltaic cells (I_{sc}, V_{co}, FF, η) were extracted from the current-voltage characteristics, allowing comparison of different cells switched on under identical conditions.

2.3.1 Short circuit current (I_{sc})

It is the current in the circuit when the load is zero. It can be achieved by connecting the positive and negative terminals by the copper wire. In practice $I_{sc} = I_{Ph}$ It varies linearly according to the solar irradiance, by canceling the voltage V in equation (2.1), we obtain:

$$I_{sc} = I_{Ph} - I_s = \left(exp\frac{I_{sc} * R_s}{A_n * k * T_c}\right) - 1) - \frac{I_{sc} * R_s}{R_{sh}} \qquad (2.2)$$

For most cells (whose series resistance is low), we can neglect the term $I_0[exp\left(\frac{Ipv * Rs}{A_n * k * T_c}\right) - 1$

In front of I_{Ph} The approximate expression of the short-circuit current is then:

$$I_{cc} \cong \frac{I_{Ph}}{1+\frac{R_5}{R_{sh}}} \quad (2.3)$$

2.3.2 Open circuit voltage (v_{0c})

It is the voltage for which the diode in the dark, provides a null current. It depends on the energy barrier and the shunt resistance; it decreases with temperature and varies little with light intensity.

$$0 = I_{sc} - I_s \left[exp^{\frac{v_{0c}}{A_n * k * T_c}} - 1 \right] - \frac{v_{0c}}{R_{sh}} \quad (2.4)$$

2.3.3 Fill factor (FF)

The fill factor FF indicates the degree of ideality of the current-voltage characteristic, so it is the ratio between the maximum output power $p_m = v_m\, I_m$ and the ideal power $v_{oc} I_{cc}$ [19].

$$FF = \frac{P_m}{v_{oc} I_{cc}} = \frac{v_m I_m}{v_{oc} I_{cc}} \quad (2.5)$$

2.3.4 PV conversion efficiency (η)

The conversion efficiency of a PV cell is a fundamental characteristic that determines its performance. It is calculated by dividing the power generated by the cell by the incident radiative power on its surface. [19].

$$\eta = \frac{P_m}{P_i} = \frac{FF \cdot v_{co} I_{cc}}{P_i} \quad (2.6)$$

P_i is the incident radiative power.

2.4 Modeling of Photovoltaic cells

2.4.1 Single-Diode-Model

This is the most commonly used model in literature is a classic one that includes a current generator to represent the incident light flux, a diode to capture the polarization phenomena, and two resistors (series and shunt) to account for the electrical characteristics.

These resistors will have some influence on the I-V characteristic of the solar cell:

- The series resistance, which primarily encompasses the resistance of the semiconductor material, the contact resistance of the collector grids, and the resistivity of these grids, represents the internal resistance of the cell.
- The shunt resistance is due to a leakage current at the junction; it depends on how it was done.

The diode current is given by:

$$I_d - I_s * \left(exp \frac{q*((V_{pv} + I_{pv} * R_s)}{A_n * k * T_c} - 1 \right) \quad (2.7)$$

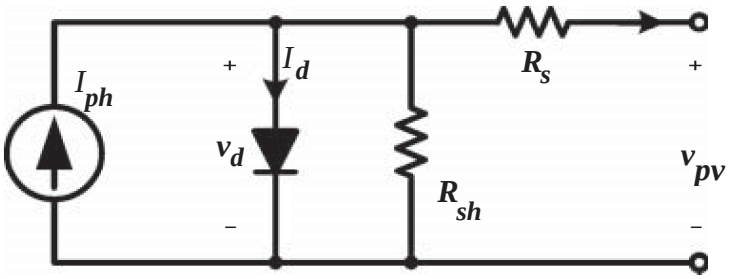

Figure 2-2: Equivalent circuit of complete single-diode CSDM [20]

The current generated by the PV cell is given by the mesh law

$$I_{pv} = I_{ph} - I_d - \frac{V_d}{R_{sh}} \quad (2.8)$$

$$I_{pv} = I_{Ph} - I_s \left(exp \frac{q*(V_{pv} + I_{pv} * R_s)}{A_n * k * T_c} - 1 \right) - \frac{V_{pv} + I_{pv} * R_s}{R_{sh}} \quad (2.9)$$

With:

I_{ph} photo current;

I_{pv} load current.

2.4.2 Simplified Single-diode Models

Besides the ISDM, the CSDM is often simplified to another two versions by neglecting either the series resistor or the shunt resistor, as shown in Figures (2-3) and (2-4).

One type of SSDM makes the series resistor, Rs equal to zero, but includes the shunt resistor R_{sh} in the equivalent circuit. The model is referred to as SSDM1, and the circuit is shown in Figure (2-3) Including one additional unknown parameter, R_{sh}, in contrast with the ISDM, the I–V expression becomes:

$$I_{pv} = I_{Ph} - I_s\left(exp^{\frac{q*V_{pv}}{A_n*k*T_c}} - 1\right) - \frac{V_{pv}}{R_{sh}} \qquad (2.10)$$

Another type of SSDM makes the shunt resistor R_{sh} equal to ∞, but includes the series resistor Rs in the model circuit. In this chapter, the model is referred to as SSDM2, and this is shown in figure (2-4) In comparison with the ISDM, the I–V expression includes an additional unknown parameter, Rs:

$$I_{pv} = I_{Ph} - I_s\left(exp^{\frac{q*V_{pv}}{A_n*k*T_c}} - 1\right) \qquad (2.11)$$

Where

$$v_d = v_{pv} + I_{pv}\,R_s \qquad (2.12)$$

The models of SSDM1 and SSDM2 are sometimes referred to as 4 parameter models because of the fourth unknown parameter: either R_{sh} or R_s. SSDM1 is considered the second choice because of its relative simplicity. SSDM2 is the last resort because of its complexity.

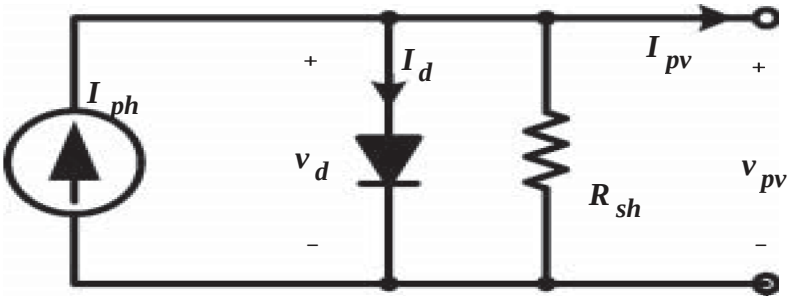

Figure 2-3:Equivalent circuit of simplified single-diode model with shunt resistor SSDM [20]

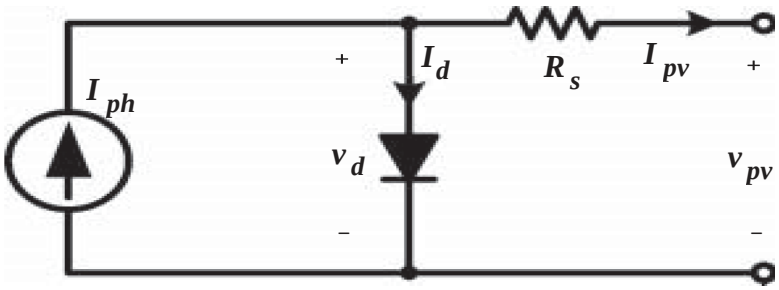

Figure 2-4 : Equivalent circuit of simplified single-diode model with series resistor SSDM2 [20]

2.4.3 The Two-Diode-Model for PV cells

A more precise model can be achieved through the Two-diode model, where two distinct diodes with different diode ideal factors (A_n) are connected in parallel. This model offers the benefit of increased accuracy; however, it also requires additional parameters for its operation.

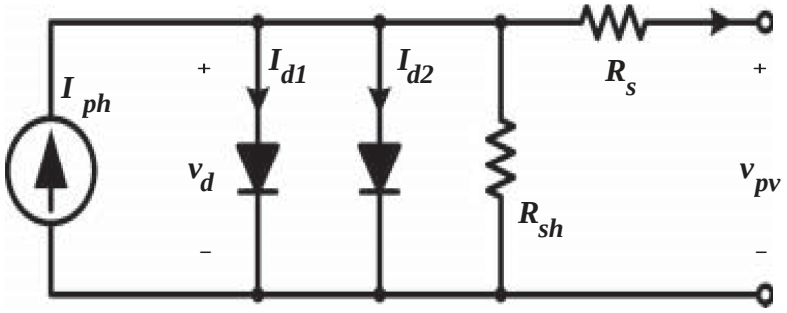

Figure 2-5: Equivalent circuit of double-diode [20]

Equation (2.1) describes the output current of the cell:

$$I_{P_v} = I_{P_h} - I_{d1} - I_{d2} - \left(\frac{v_{cpv}+I_{pv}*R_s}{R_{sh}}\right) \quad (2.13)$$

Where:

$$I_{d1} - I_{s1} - [exp\ \frac{v_{pv}+I_{pv}*R_s}{a_1*v_{pv}*T_1} - 1] \quad (2.14)$$

and

$$I_{d1} - I_{s1} - [exp\ \frac{v_{pv}+I_{pv}*R_s}{a_2*v_{pv}*T_2} - 1] \quad (2.15)$$

2.4.4 Ideal Single-diode Model

Based on the p-n junction structure for both PV cell and diode, the ideal single-diode model (ISDM) is a current source in parallel with a diode, as shown in Figure (2-6). It can be considered the simplest SDM, the series resistance and shunt resistance are removed [20].

The mathematical expressions are therefore:

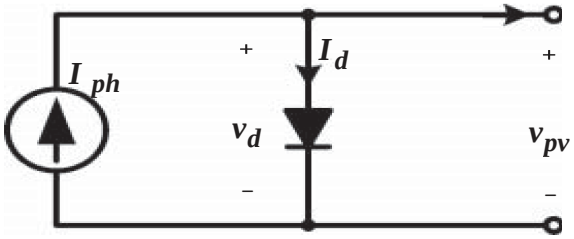

Figure 2-6: Equivalent circuits of the ideal single-diode model. [20]

$$I_{pv} = I_{Ph} - I_s\left(exp(\frac{q*V_{pv}}{A_n*k*T_c}) - 1\right) \quad (2.16)$$

When

$$I_d = I_s\left(exp\frac{(q*V_{pv})}{A_n*k*T_c} - 1\right) \quad (2.17)$$

Without the resistances, three model parameters must be identified in the modeling process: the photon current (I_{Ph}), the diode reverse bias saturation current (I_s), and the diode ideality factor (A_n).

2.4.5 Parameter Identification at Standard Test Conditions

ISDM parameters are initially determined at STC since the data are available from the product datasheet. For the case study. When the terminal of the equivalent circuit, as shown in figure (2-6) is shorted, the diode current, I_d , is equal to zero. The value of the photon current, I_{Ph}, is equal to the short-circuit current, ISCS, which is available from the product datasheet. Thus, the photon current, I_{Ph} becomes known at STC. Two unknowns remain in the ISDM to represent the diode.

When the terminal of the equivalent circuit, as shown in figure (2-6), is opened, the output current of the PV cell, I_{pv}, is equal to zero. The value of the diode current, I_d, becomes equal to the photon current, I_{Ph}, which is the Iscs at STC. This can be expressed as in (2.18), which includes two parameters of Iss and A_n:

$$I_{scs} = I_s \left(e^{\frac{(q*V_{ocs})}{A_n*VT_{ccs}}} - 1 \right) \quad (2.18)$$

Where VT_{scs} is the thermal voltage at STC, which is a constant and expressed as

$$VT_{ccs} = \frac{kT_{ccs}}{q} \quad (2.19)$$

At the MPP for STC, the I–V characteristics in (2.16) can be rewritten as (2.20), which includes two unknown parameters:

$$I_{MS} = I_{scs} - I_s \left(exp^{\frac{(V_{MS})}{A_n*VT_{cs}}} - 1 \right) \quad (2.20)$$

2.5 Simulation of a photovoltaic array with Simulink-MATLAB

2.5.1 Characteristic (I-V) with variations in solar irradiance and temperature

In fact, the characteristics (I–V) of the simulation model must meet temperature changes inside the cell and solar irradiance.

Producer Photovoltaic cells usually provide correction factors by testing experiment. Temperature coefficients for PV output current, voltage and power is αT, βT and λT, respectively. Assume that the factor of the ideal A_n is constant regardless of changes in the environment, the expression of I_{ph} should be [22]

$$I_{ph}\ (\mathrm{G}, \Delta\mathrm{T}) = \frac{\mathrm{G}}{G_{STC}} I_{SCS}\ (1 + \alpha\mathrm{T}\ \Delta\mathrm{T}) \quad (2.21)$$

Where G is the current solar irradiance and GSTC is the solar irradiance in the STS conditions. ΔT is the difference between the temperature of the T_c cell and the temperature T_cS under the STC conditions which is 25°C or 298 K. The voltage correction in open circuit for solar irradiance and cell temperature variations is given by the equation (2.22)

$$V_{oc}\ (\mathrm{G},\Delta\mathrm{T}) = V_{ocs}\ (1+\beta\mathbf{T}\Delta\mathrm{T})\ V_T \quad (2.22)$$

The value of the diode saturation current is(G,ΔT) can be determined from the open circuit conditions, since the current I_{ph} is equal to the diode current I_d:

$$I_{ph}\ (\mathrm{G},\ \Delta \mathrm{T}) = \frac{I_{ph}\ (G,\Delta T)}{\left[exp\frac{q*V_{ocs}}{A_n*k*T_c}\right]-1} \tag{2.23}$$

The equation giving the characteristics (I–V) of the photovoltaic cell with the variations of the cell temperature and solar irradiance can be written:

$$I_{pv}=I_{ph}(\mathrm{G},\Delta \mathrm{T}) - I_s\ (\mathrm{G},\Delta \mathrm{T})\ [exp\ \frac{q*V_{pv}}{A_n*k*T_c} - 1] \tag{2.24}$$

The voltage $V_{pv\mathrm{M}}$ and the current $I_{pv\mathrm{M}}$ of the photovoltaic module are given as a function of the voltage V_{pv} and current I_{pv} by the following relationships:

$$I_{pv\mathrm{M}}=N_s I_{pv} \tag{2.25}$$

$$V_{pv\mathrm{M}}=N_p V_{pv} \tag{2.25}$$

Where N_S is the number of cells in series and N_P is the number of cells in parallel. The settings of the PV cell can be estimated using the PV module specifications given in the annex Table A1.

2.5.2 Definition of SIMULINK:

Is a platform or block diagram environment used to design systems with multi-domain simulation and modeling of dynamic systems. It provides a graphical environment and a set of libraries containing blocks Modeling enables precise design, simulation, implementation and control communication and signal processing systems.

2.5.3 Block diagram

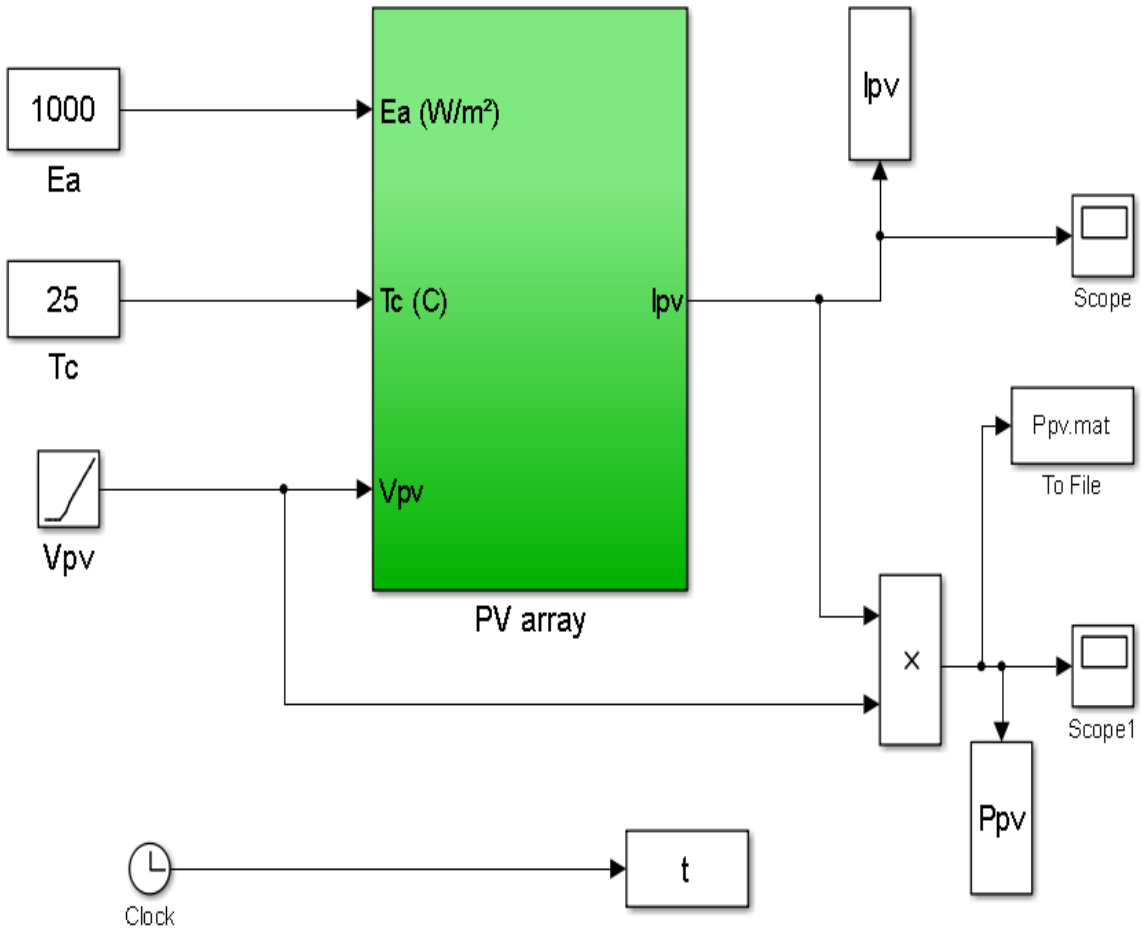

Figure 2-7: PV array simulation block diagram

2.5.4 Simulation results

2.5.4.1 Influence of solar irradiance

Figures (2-8) and (2-9) show the influence of irradiance on the characteristics of the PV panel when the irradiance changes.

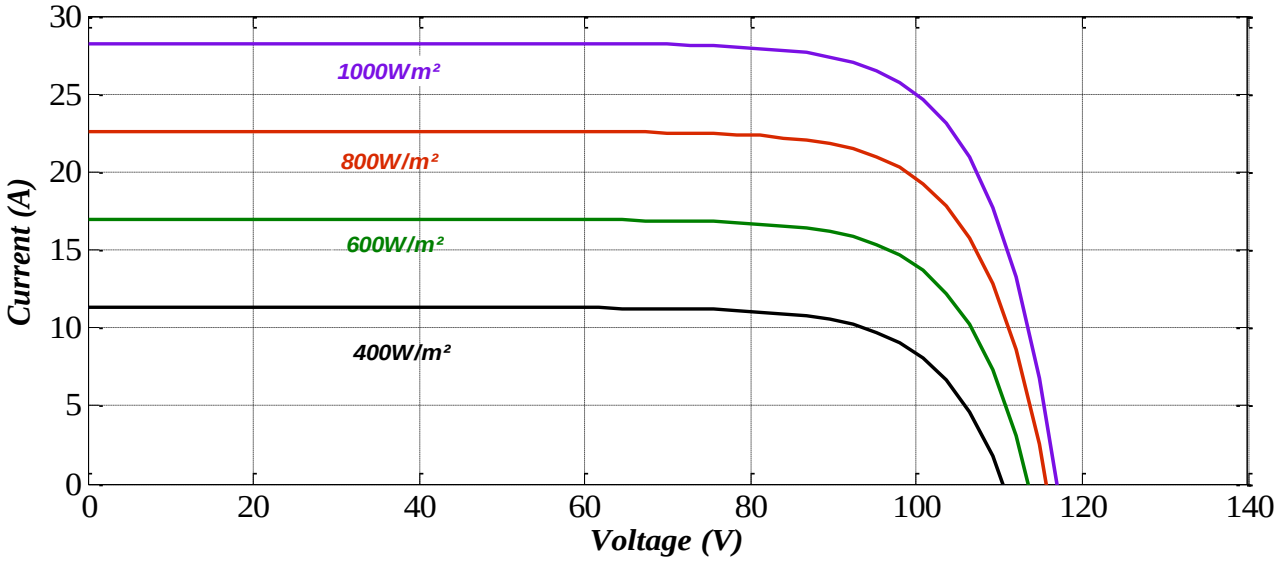

Figure 2-8:Curve I-V with constant temperature (25°C) and variable irradiance

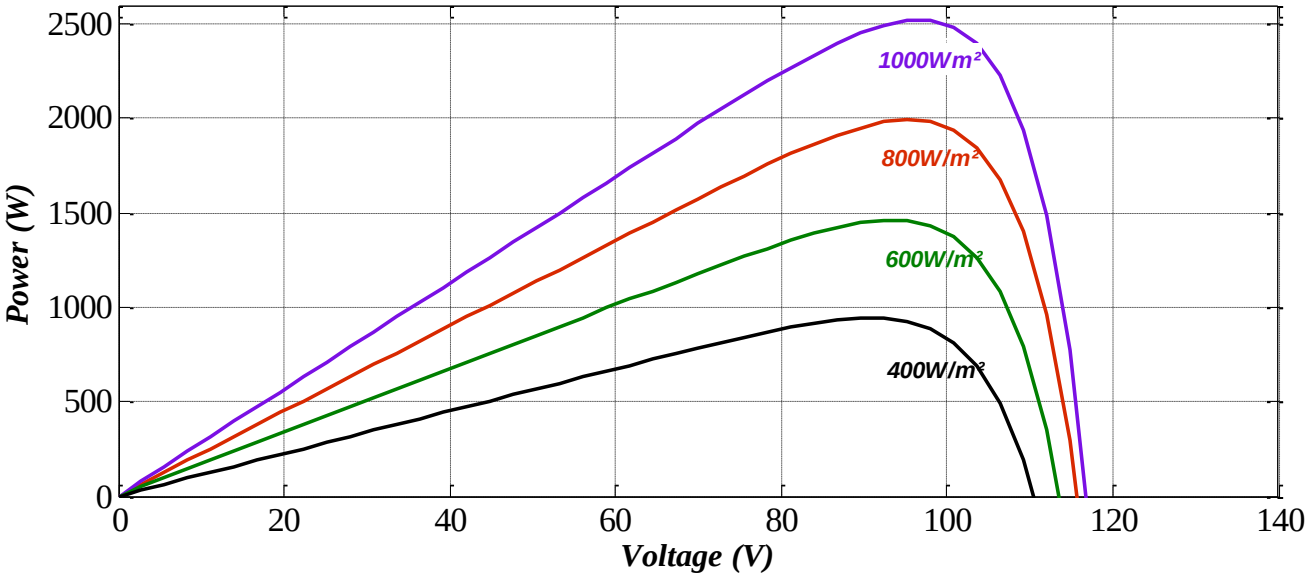

Figure 2-9: Curve P-V with constant temperature (25°C) and variable irradiance

Interpretation

By varying the solar irradiance between 400 w/m² and 1000 w/m² with a step of 200. Note that the value of the short-circuit current is directly proportional to the intensity of the solar irradiance. On the contrary, the open circuit voltage does not vary in the same proportions, it remains almost identical even in low light. The internationally accepted standard irradiance for measuring panel response photovoltaic is a solar irradiance of 1000 W/m² and a temperature of 25°C.

2.5.4.2 Influence of temperature

Figures (2-10) and (2-11) show the influence of temperature on the characteristics of the PV panel when the temperature changes.

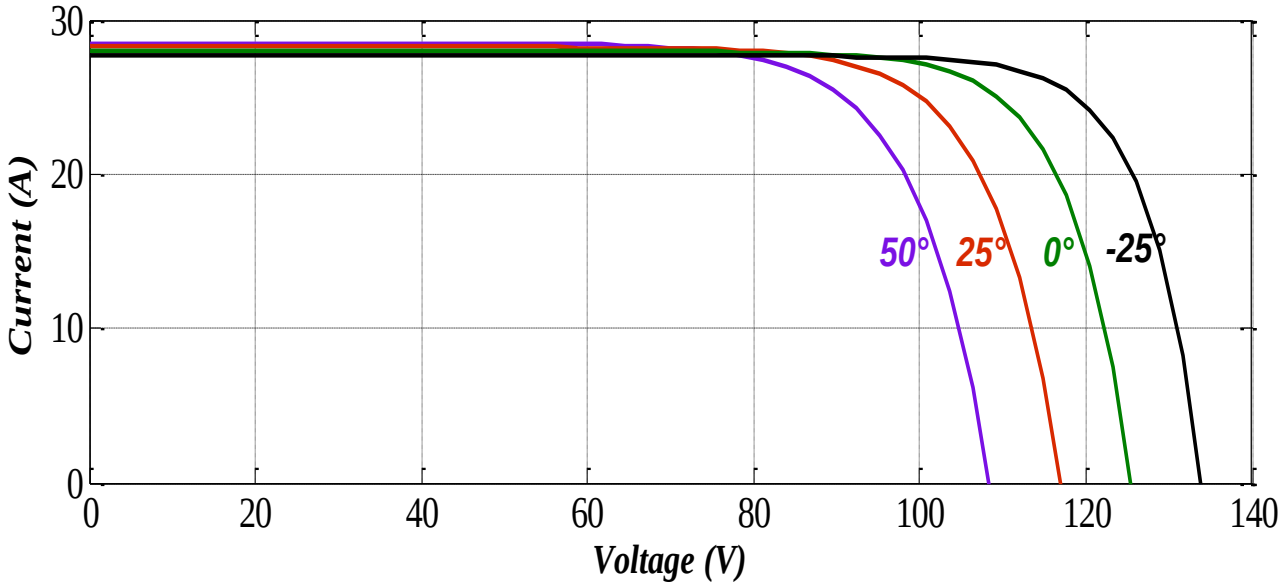

Figure 2-10: Curve I-V with constant irradiance (1000 W⁄m²) and variable temperature

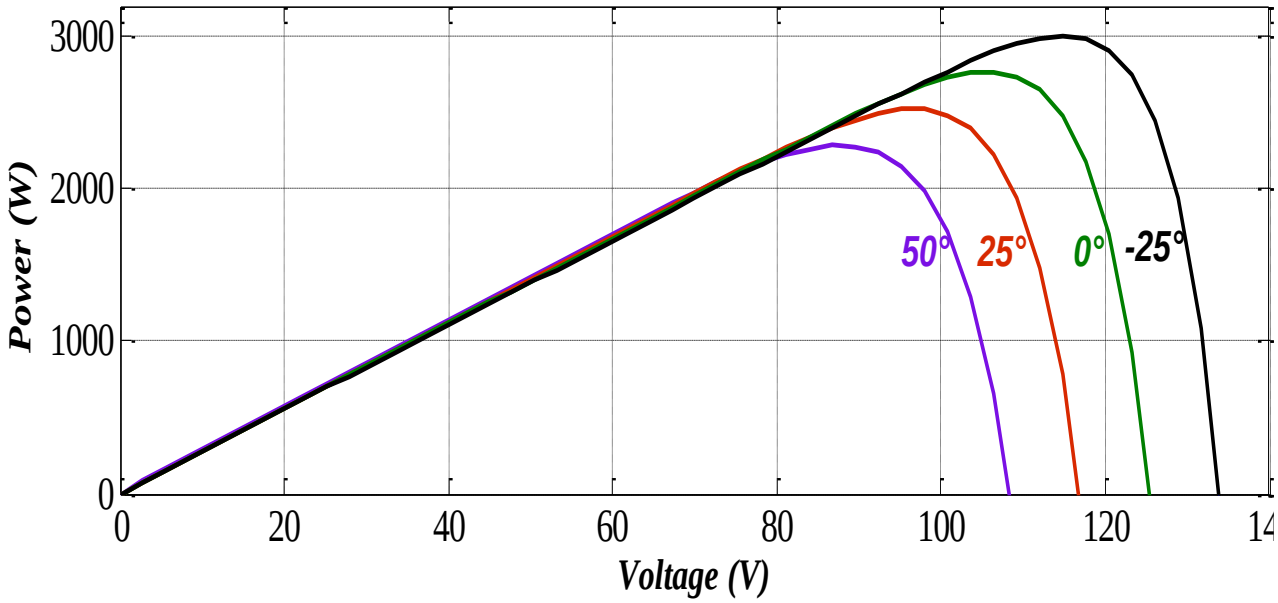

Figure 2-11: Curve P-V with constant irradiance (1000 W⁄m²) and variable temperature

Interpretation

By varying the temperature from 50°C down to -25°C. It can be seen that the temperature has a negligible influence on the value of the short-circuit current. On the other hand, the open circuit voltage drops quite sharply when the temperature increases, therefore the extractable power decreases. During the sizing of an installation, the variation in the temperature of the site must be taken into account into account.

2.6 Conclusion

In this chapter, we have presented the mathematical model of photovoltaic cells. Then we use MATLAB SIMULINK software to do it simulated on a photovoltaic panel of 9 modules with 3 × 3 configuration of nine PV modules (consisting of 60 cells connected in series) by varying solar irradiance intensity from 200W/m² to 1000W/m² with considering constant temperature of the PV panel is 25C and then, varying temperature from -25C to 50C with taking solar irradiance intensity constant 1000W/m². We have studied the effect of temperature and solar irradiance on the activity of photovoltaic cells. It is concluded that the external parameters (temperature and solar irradiance) have a big influence on the performance of the photovoltaic panel.

Chapter 3

Control and optimization of stand-alone PV system with fuzzy logic

3.1 Introduction

The ever-increasing demand for electrical energy, have greatly stimulated the search for new unlimited energy sources such as energy solar. Photovoltaic (PV) technology is based on direct conversion of irradiance solar direct current (DC) using photovoltaic cells, The scope of application of this technological innovation is very vast with different stand-alone configurations or network. The major problem with this technology (PV) lies in the design and construction of photovoltaic systems to ensure the right operation of photovoltaic modules in optimal conditions, which depend directly to climatic conditions, such as solar irradiance and temperature, these climatic variations cause the optimum power point to fluctuate. For this, between the photovoltaic generator (GPV) and the operating system, controlled static converters to extract maximum power from the generator. These commands are commonly called MPPT (Maximum Power Point Tracking). In this chapter we describe the steps for dimensioning and checking a stand-alone photovoltaic (PV) power supply system with energy storage.

The main objectives of this study are:

- The optimization of the power from the PV generator.
- Battery voltage control.
- The control of PV energy transfers to the battery (charging and unloading) and to the charge.
- Permanent control by a maximum power point tracking algorithm (MPPT)

with fuzzy logic technique.

- Controls battery charge status to avoid possible overload and discharge

3.2 Stand-alone photovoltaic system studied

Our system that we are going to study and analyze and simulate is illustrated by the equivalent circuit on the figure (3-1). The buck converter is the charge controller that transfers PV power to the battery and powers the load. The battery equivalent circuit is formed by a voltage source V_{oc} in series with a resistor R_{bat}, and an equivalent capacitance across the terminals of the battery block C_{bat}. The charging current I_{load} designates all the continuous loads connected to the battery terminals.

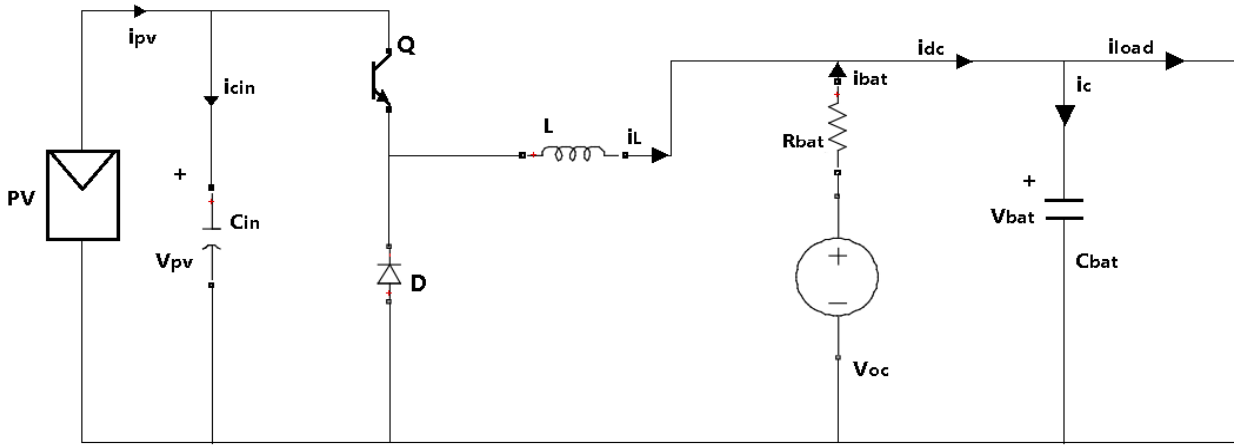

Figure 3-1: Equivalent circuit of the PV system

3.3 Sizing of DC/DC converter

The equivalent circuit of our photovoltaic system that we will study represented by figure (3-1) comprises the voltage converter DC-DC is controlled by the technique PWM (pulse width modulation), in which the duty cycle D is chosen as the system control variable.

A step-down topology must be considered if the converter output voltage is never higher than the voltage at the PV generator (V_{MPP}) terminals, when the voltage variation on both sides has been taken into account. The operating condition can be expressed as Vo (max) $\leq V_{MPP}$ (min), with Vo is the battery empty voltage, and V_{MPP} (min) means the lowest value of the voltage at the terminals of the PV generator at the MPP optimum operating point which can be estimated from the highest ambient temperature and minimum irradiance. The highest output voltage, Vo (max), can be determined from the load profile. For battery charging applications, the battery voltage becomes the output voltage of the Vo converter, which varies from the cut-off voltage at 0% of the state of charge (SOC) to the open circuit voltage which corresponds to 100% of the state of charge [23].

3.3.1 Calculation of inductance L and capacitor C in

Under standard operating conditions (STC) of temperature and solar irradiance, and at the predefined switching frequency f_{sw}, inductance ripple current and ripple voltage at the PV link must be specified by peak-to-peak, ΔI_L and ΔV_{PV} values, respectively. Steady-state analysis can determine the duty cycle at the nominal operating point. Under STC operating conditions, the photovoltaic generator should be operated in the vicinity of the optimum MPP operating point,

which is represented by V_{MPP} voltage and I_{MPP} current. The duty cycle can be calculated by the formula:

$$D_0 = \frac{V_{0-NOM}}{V_{MPP}} \tag{3.1}$$

The nominal voltage $V_{O\text{-}NOM}$ corresponding to the continuous operation mode of the converter (CCM) can be specified from the load profile. The value of inductance, L, and capacity, C_{in}, can be calculated using equations (3.2) and (3.3), respectively [24].

$$L = \frac{V_{0-NOM}(1-D_0)}{\Delta I_L f_{sw}} \tag{3.2}$$

$$C_{in} = \frac{I_{MPP}(1-D_0)}{\Delta V_{pv} f_{sw}} \tag{3.3}$$

3.4 Modelling and simulation of Buck converter

In this analysis, we will focus on a converter that utilizes ideal switching devices operating with a switching period T and a duty cycle D. By applying Kirchhoff's voltage law to the inductance loop and Kirchhoff's current law to the node connected to the capacitor branch, the state equations corresponding to the converter in continuous conduction mode (CCM) can be comprehended effortlessly. Based on the switching device conduction state Q, we distinguish two cases:

Q on-state Dynamics:

$$\begin{cases} \frac{di_L}{dt} = \frac{1}{L}(V_{in} - v_o) \\ \frac{dv_o}{dt} = \frac{1}{C}(i_L - \frac{v_o}{R}) \end{cases}, \quad 0 < t < dT, \quad Q: ON \tag{3.4}$$

Q off-state Dynamics:

$$\begin{cases} \frac{di_L}{dt} = \frac{1}{L}(-v_o) \\ \frac{dv_o}{dt} = \frac{1}{C}(i_L - \frac{v_o}{R}) \end{cases}, \quad dT < t < T, \quad Q: OFF \tag{3.5}$$

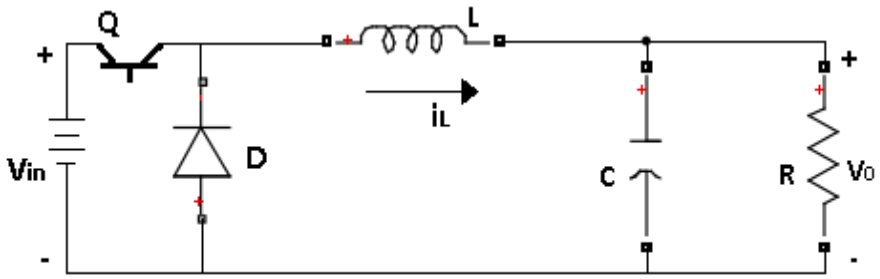

Figure 3-2 : Buck converter

These equations are implemented in Simulink as shown in the block diagram of figure (3-3)

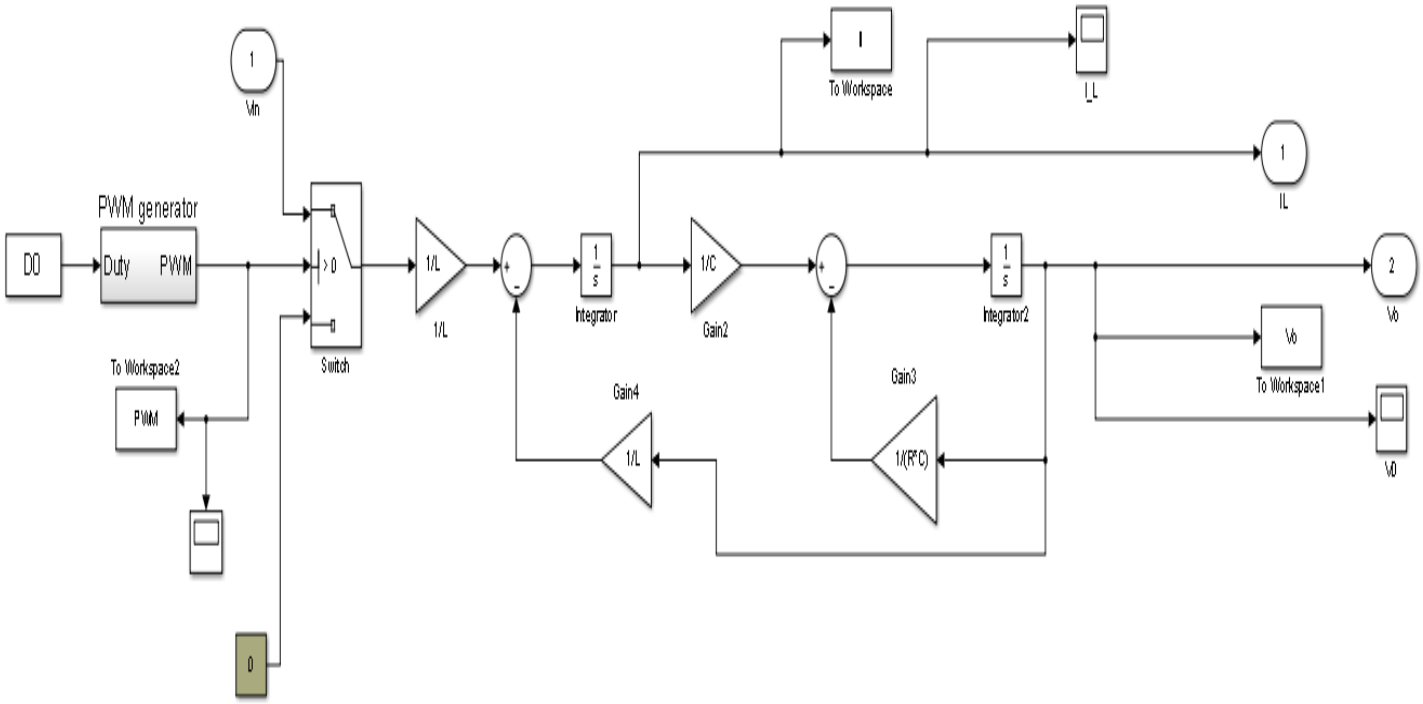

Figure 3-3: Open loop buck converter simulation block diagram

3.5 Simulation results

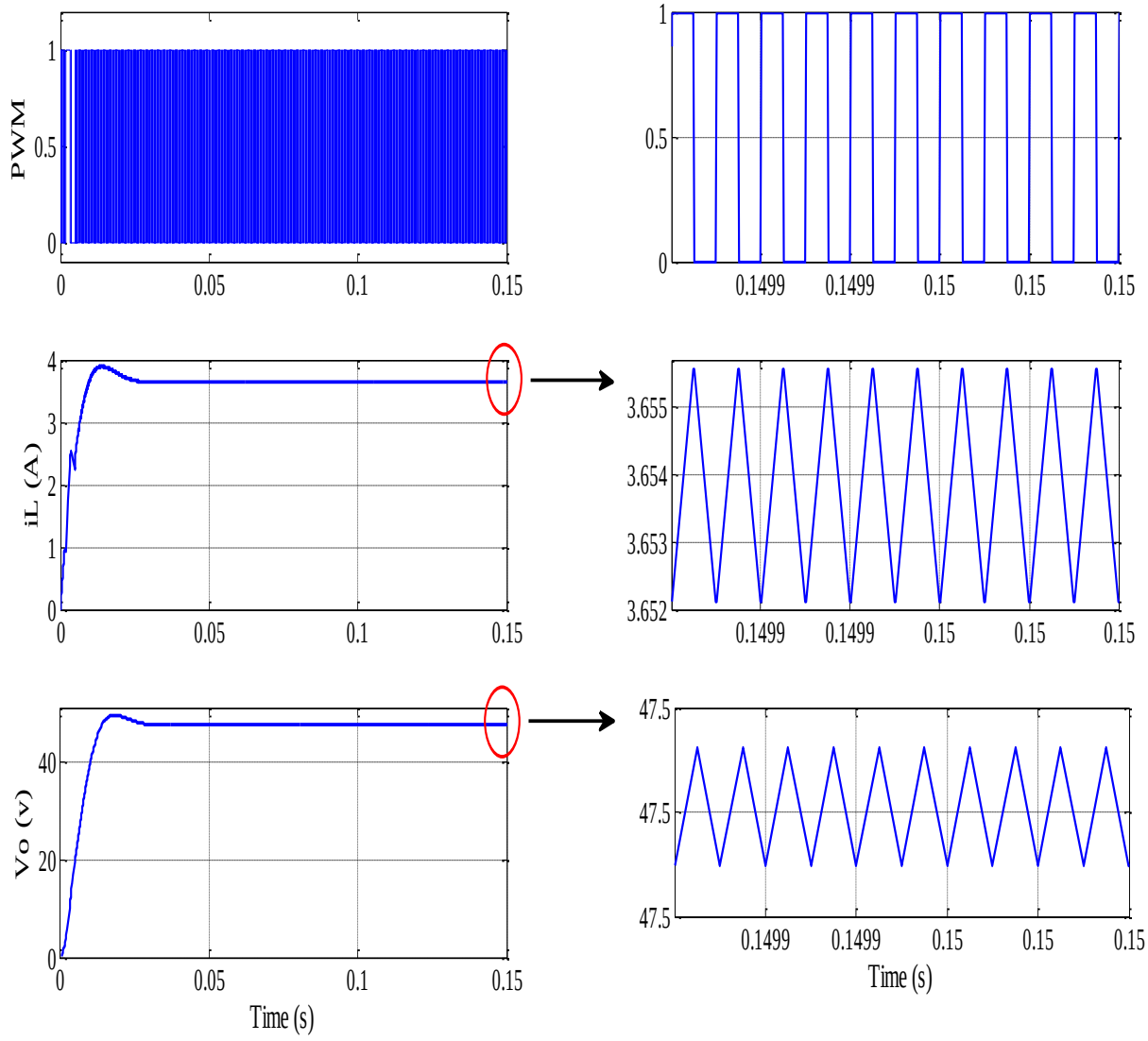

Figure 3-4: Open loop buck converter simulation block diagram

Vin=95V, L=167mH, C=272µF, R=13Ω, f=50KHz, Vo=48V

3.6 Dynamic modeling of the photovoltaic system

The PV generator and power conditioning circuits exhibit nonlinearity. By considering the dynamic behavior of the ON/OFF switching state, an averaged model can be obtained using the state-space averaging method, along with the linearization technique to derive linear models for dynamic analysis and regulator synthesis. This method relies on the assumption that the switching device frequency is significantly higher than the critical dynamics of the system, which primarily involve energy storage components like capacitors and inductors. Under this condition, the nonlinear dynamics associated with switching can be disregarded for the purposes of dynamic

analysis and controller synthesis. During a switching cycle, the state space model of the system can be derived from the ON/OFF state of switch Q.

The average value of the continuous signals can be used to form a dynamic model without need to represent switching ripples. The dynamics of the system can be represented in a general form that describes the behaviors of the inductor current and PV link voltage [23].

$$\frac{di_L}{dt} = f(i_L, v_{pv}, d) \tag{3.6}$$

$$\frac{dv_{pv}}{dt} = g(i_L, v_{pv}, d) \tag{3.7}$$

3.7 The linear model can be derived by a linearization process

$$\frac{d\tilde{i}_L}{dt} = \left.\frac{\partial f}{\partial v_{pv}}\right|_{SS} \tilde{v}_{pv} + \left.\frac{\partial f}{\partial i_L}\right|_{SS} \tilde{i}_L + \left.\frac{\partial f}{\partial d}\right|_{SS} \tilde{d} \tag{3.8}$$

$$\frac{d\tilde{v}_{pv}}{dt} = \left.\frac{\partial g}{\partial v_{pv}}\right|_{SS} \tilde{v}_{pv} + \left.\frac{\partial g}{\partial i_L}\right|_{SS} \tilde{i}_L + \left.\frac{\partial g}{\partial d}\right|_{SS} \tilde{d} \tag{3.9}$$

Where $\tilde{v}_{pv}$, $\tilde{i}_L$, $\tilde{d}$ and represent the small steady state signals (SS) of the PV module voltage V_{pv}, the inductor current i_L and the duty cycle d.

$$\frac{di_L}{dt} = \underbrace{\frac{1}{L}\left[dv_{pv} - v_O\right]}_{f(v_{pv}, d, i_L)} \tag{3.10}$$

$$\frac{dv_{pv}}{dt} = \underbrace{\frac{1}{C_{in}}\left[di_{pv} - di_L\right]}_{g(v_{pv}, d, i_L)} \tag{3.11}$$

Where the switching duty cycle d is the control variable. Due to the nonlinear characteristics of (3.10) and (3.11), linearization is required to derive the small-signal model at the nominal operating point. In the predefined steady state, the small-signal model can be derived using equations (3.8) and (3.9), and expressed as a state space by equation (3.12):

$$\begin{bmatrix} \frac{d\tilde{i}_L}{dt} \\ \frac{d\tilde{v}_{pv}}{dt} \end{bmatrix} = \begin{bmatrix} 0 & \frac{D}{L} \\ -\frac{D}{C_{in}} & \frac{1}{R_{pv}C_{in}} \end{bmatrix} \begin{bmatrix} \tilde{i}_L \\ \tilde{v}_{pv} \end{bmatrix} + \begin{bmatrix} \frac{v_{pv}}{L} \\ -\frac{i_L}{C_{in}} \end{bmatrix} \tilde{d} \qquad (3.12)$$

Where D, V_{pv} and i_L are considered constant in steady state. The signals, are the state variables and $\tilde{d}$ represents the control variable, R_{pv} is the resistance of the PV module defined as the ratio between the voltage and the current of the PV terminal.

3.8 Battery modeling

The battery can be thought of as a variable voltage source, with the steady state value being affected by the state of charge (SOC) and rate of charge or discharge. The battery can be represented by a simplified model using a Thevenin equivalent circuit, consisting of a voltage source in series with a resistor, as depicted in figure (3-1). Equation (3.13) describes the model that can simulate the steady-state voltage response to changes in the discharge current.

$$v_{bat} = V_{OC} - R_{bat}.i_{bat} \qquad (3.13)$$

BK-10V10T is a specific battery module used in the studied stand-alone photovoltaic system. These parameters are defined in Table. Figure (3-5) illustrates the discharge characteristics given by the product data sheet [25].

For a general representation, discharge capacity, Cdis can be converted to state of charge (SOC), which is the normal way to represent battery capacity.

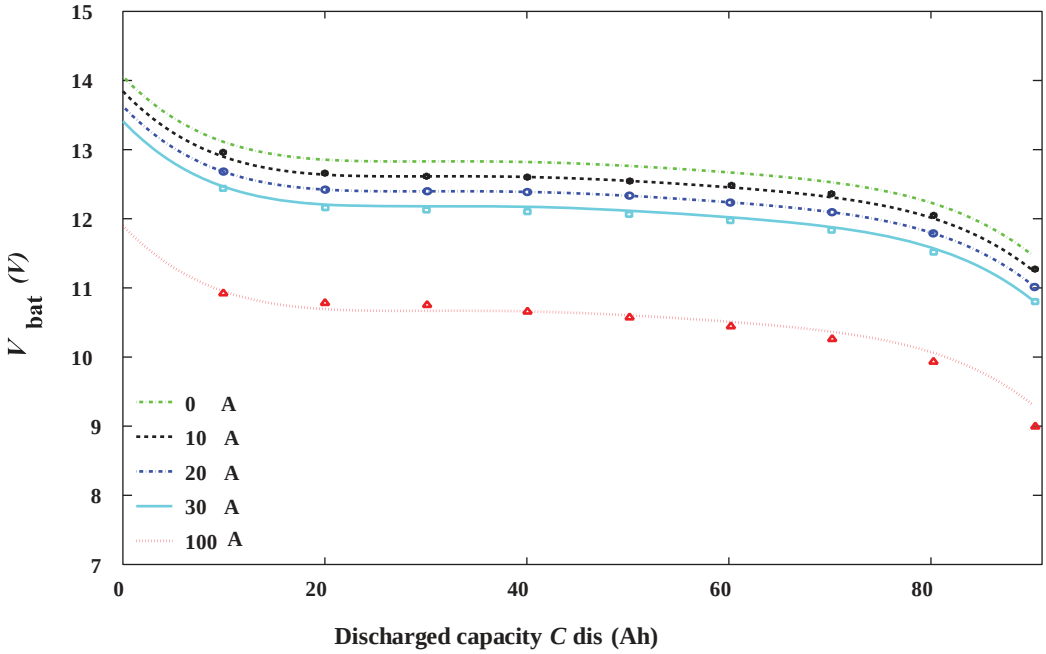

Figure 3-5: Battery voltages according to discharge capacity [25].

For the BK-10V10T module, the polynomial function is derived in equation (3.14), where the polynomial constants are listed in Table A3 of the Annexes.

$$V_{OC} = P_{S5}SOC^5 + P_{S4}SOC^4 + P_{S3}SOC^3 + P_{S2}SOC^2 + P_{S1}SOC + P_{S0} \quad (3.14)$$

In the equivalent circuit of figure (3-1), the inductance current of the buck converter is denoted i_L. The dynamics of the circuit is given by the equations:

$$i_L + i_{bat} = C_{BAT}\frac{dv_{bat}}{dt} + i_{load} \quad (3.15)$$

$$R_{bat}C_{BAT}\frac{di_{bat}}{dt} + i_{bat} = i_{load} - i_L \quad (3.16)$$

With the assumption of a constant voltage V_{oc} in steady state, the dynamics of the battery connection can be represented by the transfer function:

$$i_{bat}(s) = \frac{i_{load} - i_L}{R_{bat}C_{BAT}s + 1} \quad (3.17)$$

3.8.1 The battery simulation block diagram

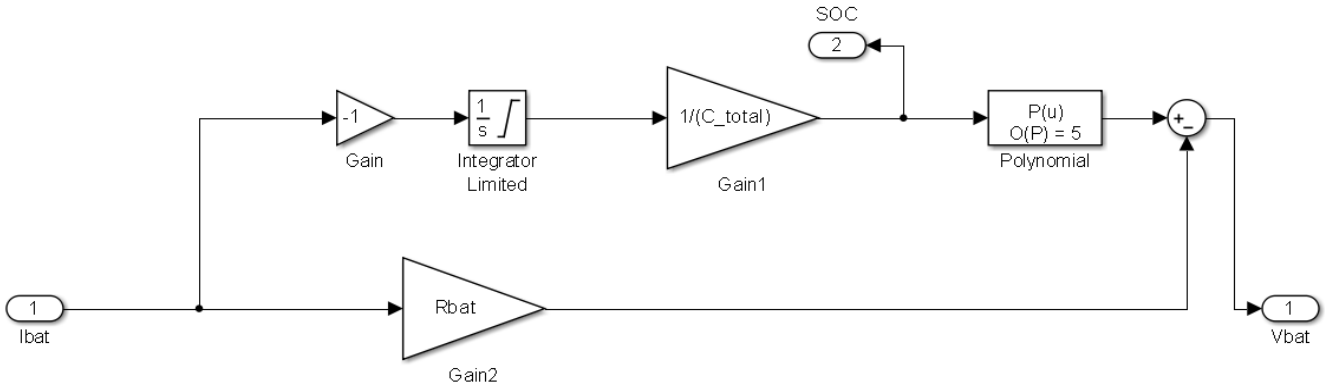

Figure 3-6: Battery simulation block diagram

3.8.2 Battery voltage regulation

We derive from equation (3.12) the following transfer function:

$$\frac{\tilde{v}_{pv}(s)}{\tilde{d}(s)} = \frac{-\frac{i_L}{C_{in}}s - \frac{Dv_{pv}}{LC_{in}}}{s^2 - (\frac{1}{R_{pv}C_{in}})s + \frac{D^2}{LC_{in}}} \tag{3.18}$$

The transfer function in equation (3.18) represents a second-order system, which can be normalized by equation (3.19):

$$G_0(s) = \frac{k_0(\beta s + 1)}{s^2 + 2\xi\omega_n s + \omega_n^2} \tag{3.19}$$

Where the undamped natural frequency and the damping factor are expressed as ωn and ξ respectively. We can then derive the coefficients relating to the equation (3.18):

$$\omega_n = \frac{D}{\sqrt{LC_{in}}} \tag{3.20}$$

$$\xi = -\frac{\sqrt{L}}{2DR_{pv}\sqrt{C_{in}}} \tag{3.21}$$

$$k_0 = -\frac{Dv_{pv}}{LC_{in}} \tag{3.22}$$

$$\beta = \frac{Li_L}{Dv_{pv}} \tag{3.23}$$

We suggest using a standard PID controller to regulate the PV link voltage. A first-order desired closed-loop transfer function F(s) is adopted, with the general form:

$$F(s) = \frac{1}{\alpha s + 1} \tag{3.24}$$

α is a constant to be defined. The regulator can then be derived by expression (3.25):

$$C(s) = \frac{s^2 + 2\xi\omega_n s + \omega_n^2}{k_0 s(\alpha\beta s + \alpha + \beta)} \tag{3.25}$$

The PID regulator defined by the transfer function (4.27) can be written in the following parallel form:

$$C(s) = k_p + \frac{k_i}{s} + \frac{k_d}{\tau.s + 1} \tag{3.26}$$

The PID controller parameters can be derived from equations (3.25) and (3.26).

$$\tau = \frac{\alpha.\beta}{\alpha + \beta} \tag{3.27}$$

$$k_i = \frac{\omega_n^2}{k_0(\alpha + \beta)} \tag{3.28}$$

$$k_p = \frac{2\zeta\omega_n(\alpha + \beta) - \omega_n^2\alpha\beta}{k_0(\alpha + \beta)^2} \tag{3.29}$$

$$k_d = \frac{(\alpha + \beta)^2 - 2\zeta\omega_n(\alpha + \beta)\alpha\beta + \omega_n^2\alpha^2\beta^2}{k_0(\alpha + \beta)^3} \tag{3.30}$$

3.9 Power Maximization Algorithm (MPPT)

For the photovoltaic system to operate at maximum power points of their characteristics, there are specific control laws that meet this need. This command is called in the literature "Search for the Maximum Power Point" (MPPT). The objective of these commands is to search for the maximum power point (MPP) while maintaining a good impedance match between the generator and the load, ensuring the maximum power transfer. The MPPT command, also known as "Maximum Power Point Tracking," is a crucial command for the optimal operation of the photovoltaic system. The control principle relies on automatically adjusting the duty cycle to its optimum value, thereby maximizing the power output from the PV panel..

In this chapter, we will use the technique of fuzzy logic to optimize the operation of the photovoltaic system. The figure (3-7) represents an elementary photovoltaic conversion chain associated with an MPPT command.

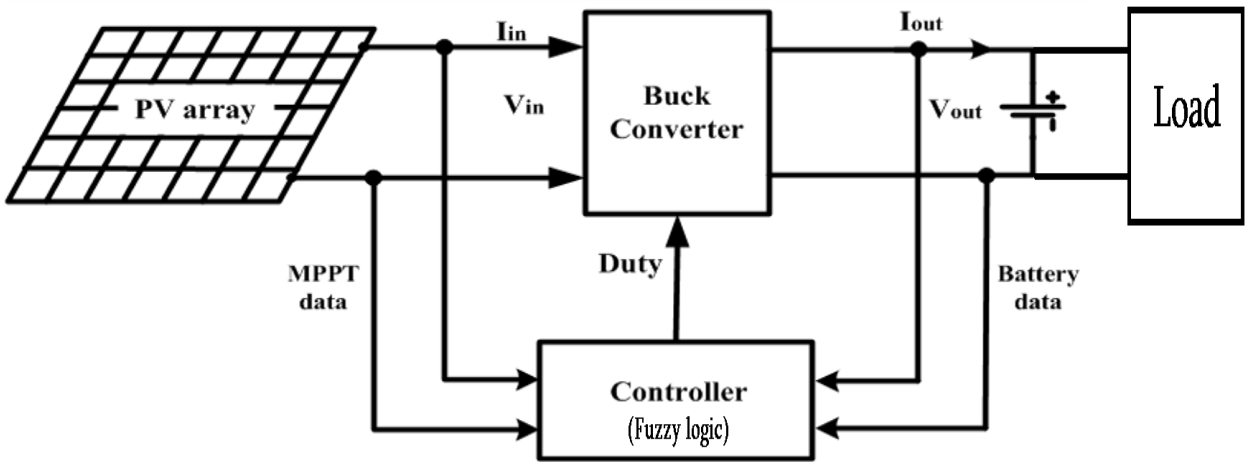

Figure 3-7: Synoptic diagram of a photovoltaic system with MPPT

3.10 General overview of fuzzy logic technique

3.10.1 Fuzzy logic definition

Fuzzy logic (FL) is an alternative approach to Boolean logic that focuses on handling degrees of truth instead of strict binary values. It was initially introduced by Professor L. Zadeh in 1965 and offers a way to address complex and unfamiliar systems. Traditional methods often fall short when dealing with such systems, particularly those that are nonlinear and intricate, and they struggle to produce satisfactory outcomes. In contrast, FL systems are more adaptable compared

to classical and conventional methods. They excel at modeling and approximating nonlinear systems, providing desirable results [26].

Fuzzy logic systems are designed around transforming control linguistics into if-then statements within an automated control system. In these systems, having a solid understanding and experience can prove to be more valuable than solely relying on technical knowledge and comprehending the intricacies of system models [27-28].

Fuzzy logic or fuzzy set theory is a new method of MPPT control to obtain the maximum power point (MPP). The fuzzy controller works in two basic modes coarse and fine [29]. This control algorithm consists of three steps, namely:

• Fuzzification

• The inference method

• Defuzzification

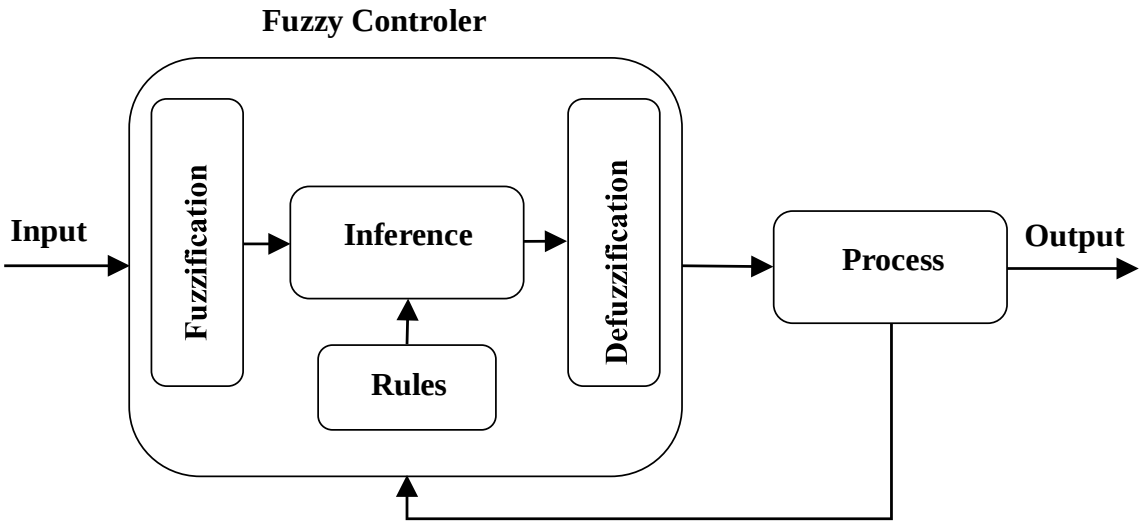

Figure 3-8: Block diagram for a fuzzy controller [30]

3.10.1.1 Fuzzification

The fuzzification module is responsible for transforming real-valued variables into fuzzy variables [31]. It is the process of converting crisp (exact) input values into fuzzy values by determining the degree of membership of each input value in the corresponding fuzzy sets. It involves evaluating the input values' similarity to each fuzzy set and assigning membership degrees accordingly.

The membership functions for each fuzzy subset are represented using different shapes (triangle, trapezoid...), implying that a given input value is predominantly associated with one fuzzy subset. The input error (e) for the fuzzy logic controller is calculated based on the maximum power point, although the exact calculation method or formula is not provided in the given information [32].

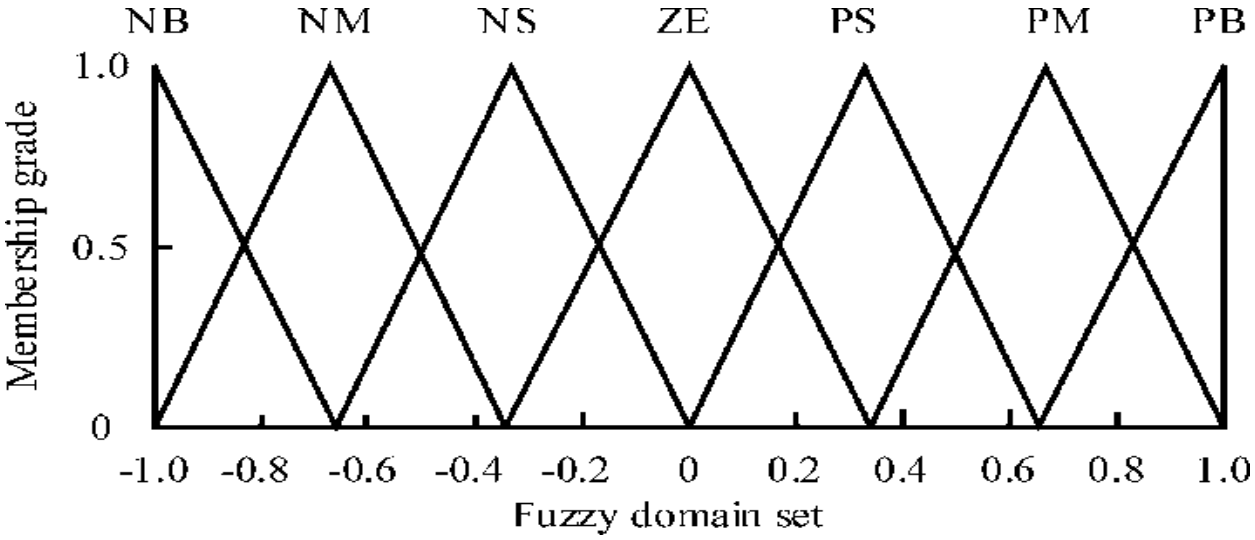

Figure 3-9 : Fuzzy logic control membership function for input and output [32]

3.10.1.2 Inference methods

In fuzzy logic, inference methods are employed to make conclusions or decisions by utilizing fuzzy inputs and a set of predefined fuzzy rules. These methods entail combining the fuzzy inputs, applying fuzzy logic operators, and there are several inference methods are commonly used to draw conclusions or make decisions based on fuzzy inputs and predefined fuzzy rules. Here are some widely employed inference methods in fuzzy logic:

- The Mamdani method is a popular and extensively employed inference technique in fuzzy logic. It entails the utilization of fuzzy logic operators, such as conjunction (AND), disjunction (OR), and implication, to combine fuzzy inputs and activate pertinent rules. The output generated by the Mamdani method is a fuzzy set, which is usually defuzzied to obtain a crisp output [33].
- The Sugeno method, which is also referred to as the Takagi-Sugeno-Kang (TSK) method, distinguishes itself from the Mamdani method in its rule structure and output representation.

Unlike the Mamdani method, which produces fuzzy sets as outputs, the Sugeno method generates crisp outputs using weighted average or mathematical functions. In the Sugeno method, each rule is associated with a linear function, and the final output is determined by combining the outputs of all activated rules [34].

- Tsukamoto Method: The Tsukamoto method is another popular inference method in fuzzy logic. It uses fuzzy logic operators and a specific form of rule interpolation to determine the degree of activation for each rule. The output of the Tsukamoto method is a fuzzy set, which is typically defuzzied to obtain a crisp output [35].
- Larsen Method: The Larsen method is an inference method that uses fuzzy logic operators and a specific form of rule aggregation. It applies a scaling factor to the consequent part of each rule based on the degree of activation, resulting in a weighted output. The aggregated outputs from all activated rules are combined to obtain a final output [36].

These are just a few examples of inference methods in fuzzy logic. Other methods, such as the fuzzy min-max method, hybrid methods, and fuzzy neural networks, have also been developed and utilized in specific applications. The choice of inference method depends on the nature of the problem, the desired output representation, and the specific requirements of the application.

3.10.1.3 Defuzzification

The defuzzification module in the fuzzy logic controller converts the linguistic results obtained from the inference engine into a crisp output value [37]. That value can be used for decision-making or action-taking. Defuzzification methods determine a single numerical value that best represents the overall information conveyed by the fuzzy set, such as the centroid, weighted average, or maximum membership value. The defuzzied output provides a precise result from the fuzzy logic system.

3.11 Fuzzy logic applied to our system

3.11.1.1 Fuzzy Logic MPPT method

The input variables considered in this paper are the change in PVG power (ΔP_{PV}) and photovoltaic voltage (ΔV_{PV}), while the output variable is the change in PV reference voltage (ΔV_{ref}). These variables are calculated using the following equations**:**

$$\begin{cases} \Delta P = P(k) - P(k-1) \\ \Delta V = V(k) - V(k-1) \\ V(k)_{ref} = V(k-1) + \Delta V_{ref} \end{cases} \quad (3.31)$$

Where:

k is the sampling time,

P(k) is the actual PVG power,

V(k) is the corresponding instantaneous voltage.

During the fuzzification process, numerical input variables are transformed into linguistic variables that can assume specific membership function values. These values, as outlined in Table (3-1), include NB (Negative Big), PB (Positive Big), NM (Negative Medium), PM (Positive Medium), NS (Negative Small), PS (Positive Small), and ZE (Zero).

Table (3-1) presents the rule base of the fuzzy logic controller, specifying the relationships between the input variables and the corresponding fuzzy sets [32].

ΔV_{ref}	**ΔP_{PV}**							
ΔV_{PV}		NB	NM	NS	Z	PS	PM	PB
	NB	PB	PB	PM	Z	NM	PB	NB
	NM	PB	PM	PS	Z	NS	NM	NB
	NS	PM	PS	PS	Z	NS	NS	NM
	Z	NB	NM	NS	Z	PS	PM	PB
	PS	NM	NS	NS	Z	PS	PS	PM
	PM	NB	NM	NS	Z	PS	PM	PB
	PB	NB	NB	NM	Z	PM	PB	PB

Table 3-1 : Fuzzy rules

The fuzzy logic structure applied in our system is represented in figure (3-10)

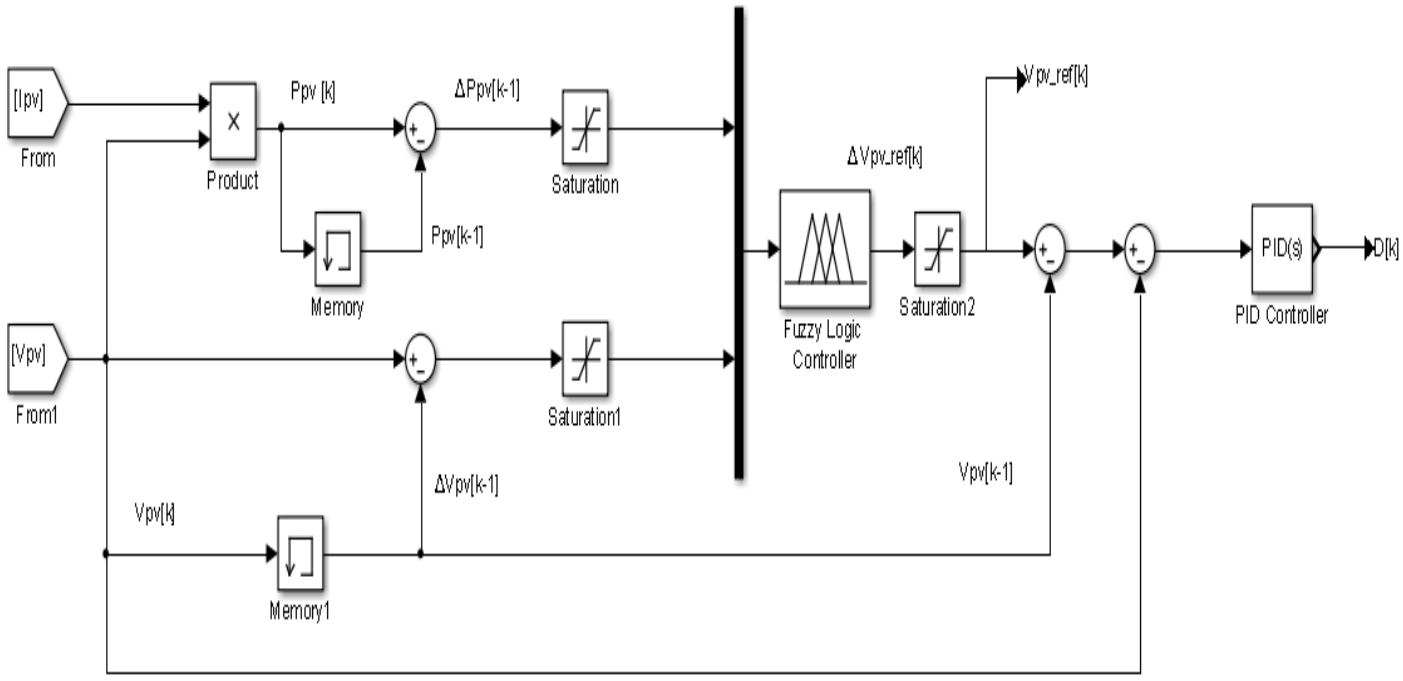

Figure 3-10 : Fuzzy logic MPPT structure

3.11.1.2 Integration of battery charge control with MPPT

To prevent PV generation in case of battery load capacity overload, the charging cycle must be maintained using the MPPT function. When the battery voltage and current reach the charging limits, the MPPT algorithm should be stopped to reduce PV energy production. Figure (3-11) illustrates the integration of battery charge control and the MPPT algorithm. The permissible voltage limits for the battery, lower (V_{min}) and upper (V_{max}), are given in the appendix table A2.

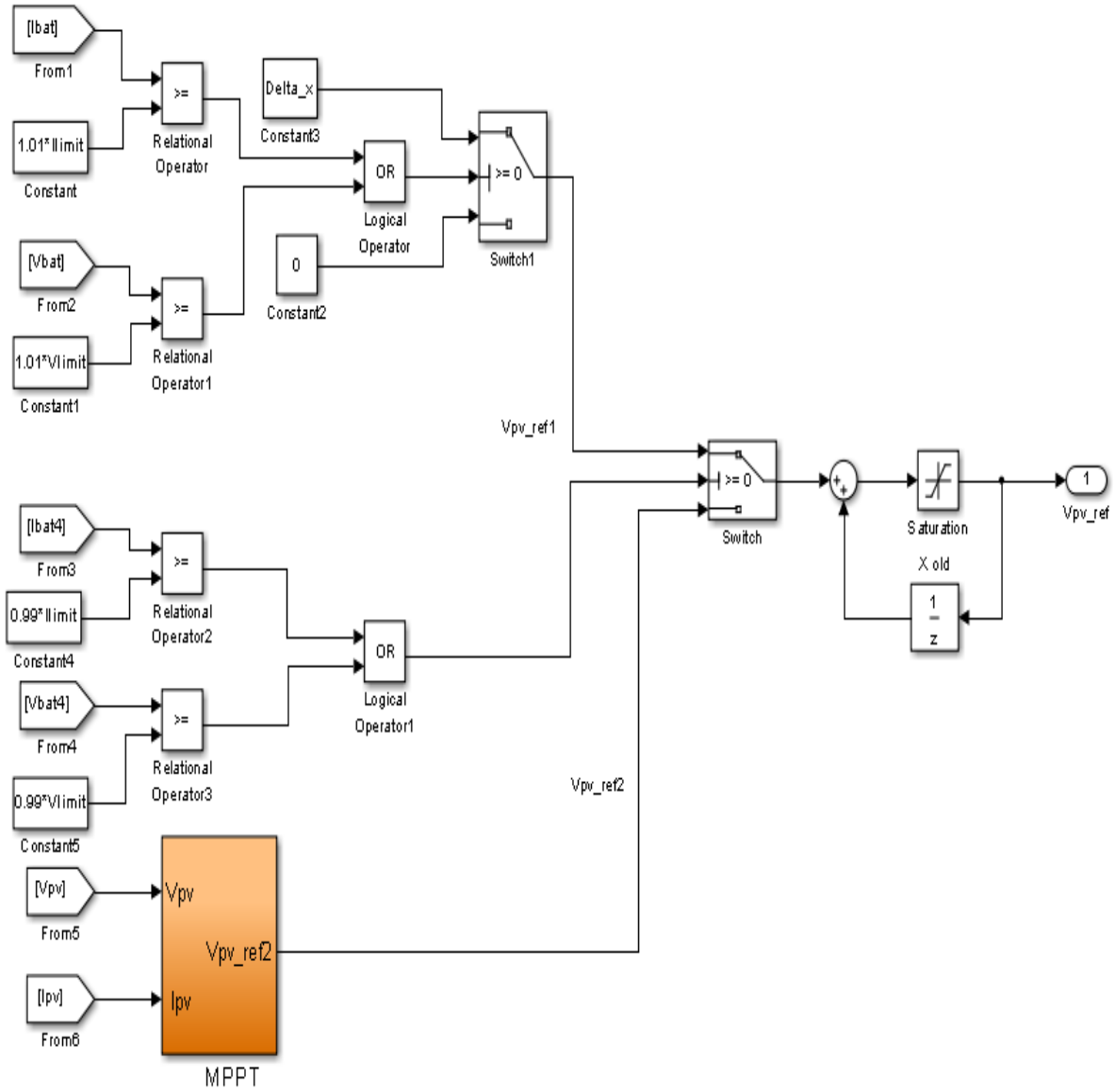

Figure 3-11: Integration of battery charge control with MPPT

3.12 Simulation results

The global simulation model of the studied system is presented in figure (3-12); It comprises the photovoltaic generator, the DC/DC buck converter, the battery, with the control blocks and MPPT with the fuzzy logic technique. The photovoltaic panel settings are given in the appendix table A1.

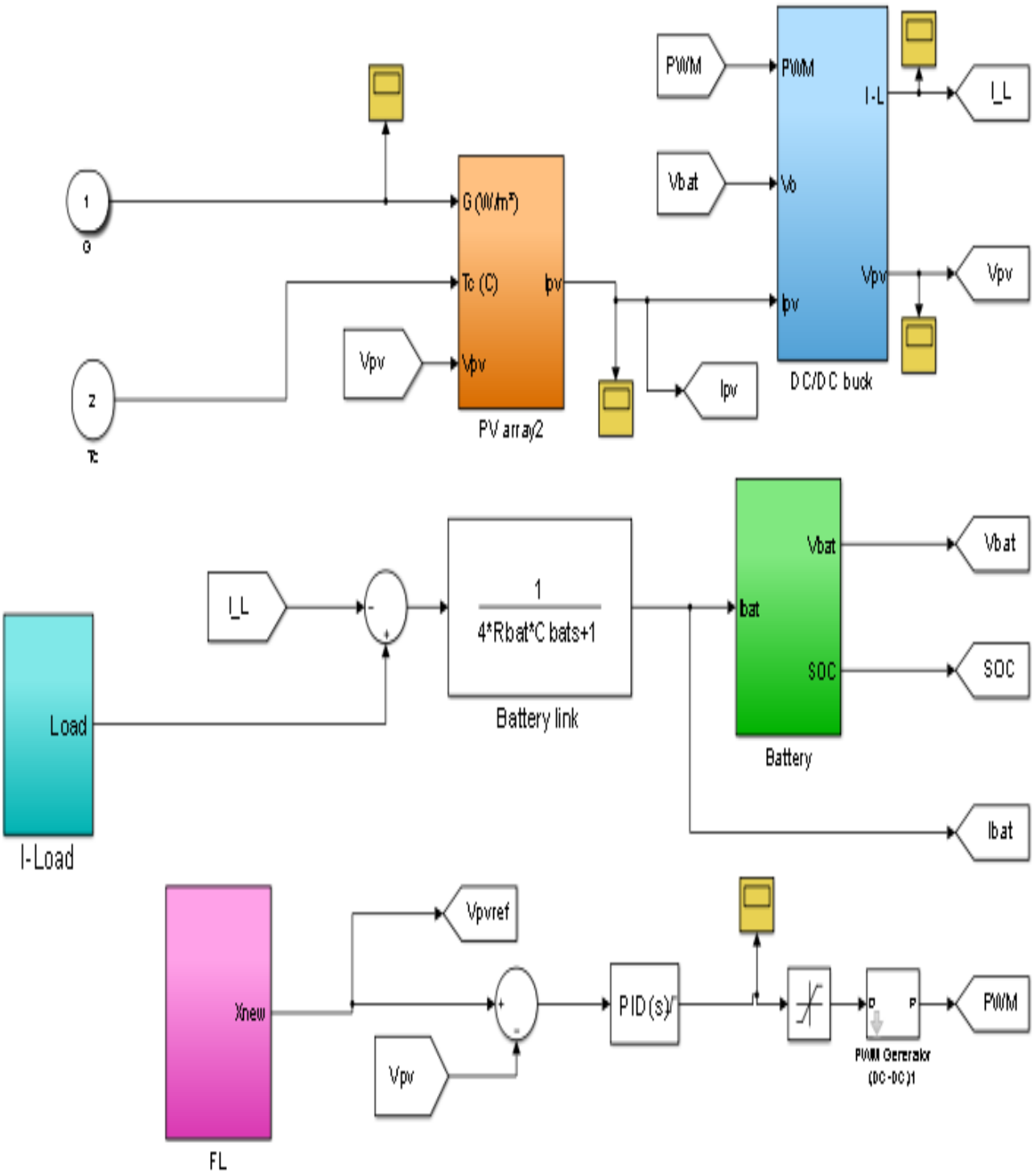

Figure 3-12: Stand-alone PV system simulation model

To validate the model, we will analyze three scenarios:

3.12.1 Scenario N° 1 : Solar irradiance variations

The solar irradiance is varied according to the figure (3-13); while maintaining the temperature and the load.

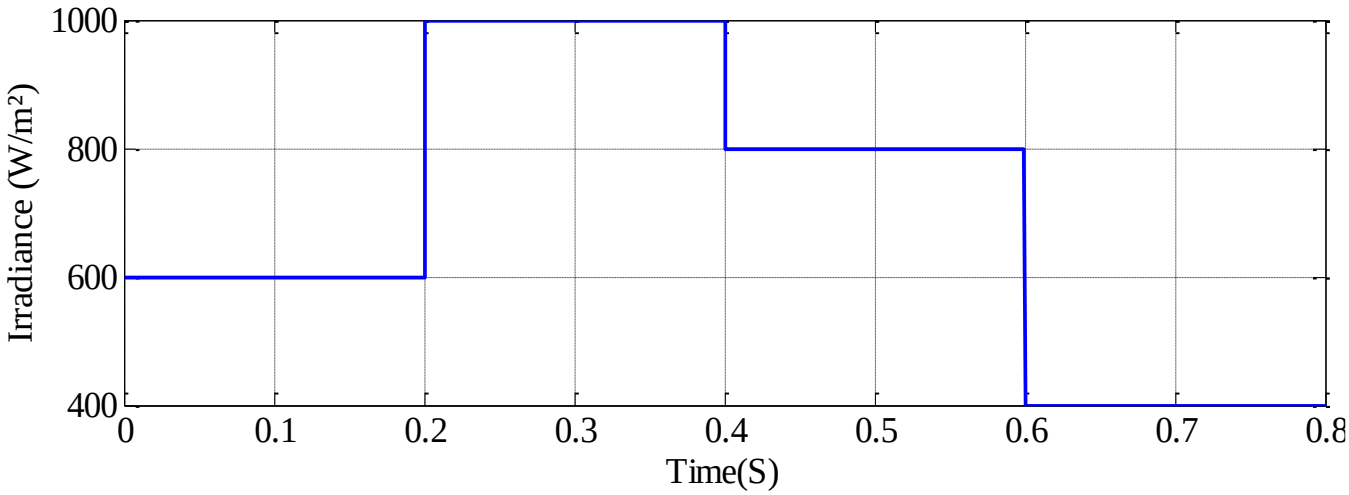

Figure 3-13 : Solar irradiance curve

Figure (3-13) represent that we changed the solar irradiance from 400 (W/m²) to 1000 (W/m²) in a step of 200 (W/m²) in order to see the solar irradiance effect. The solar irradiance influences the rest despite we fixed the temperature and the load.

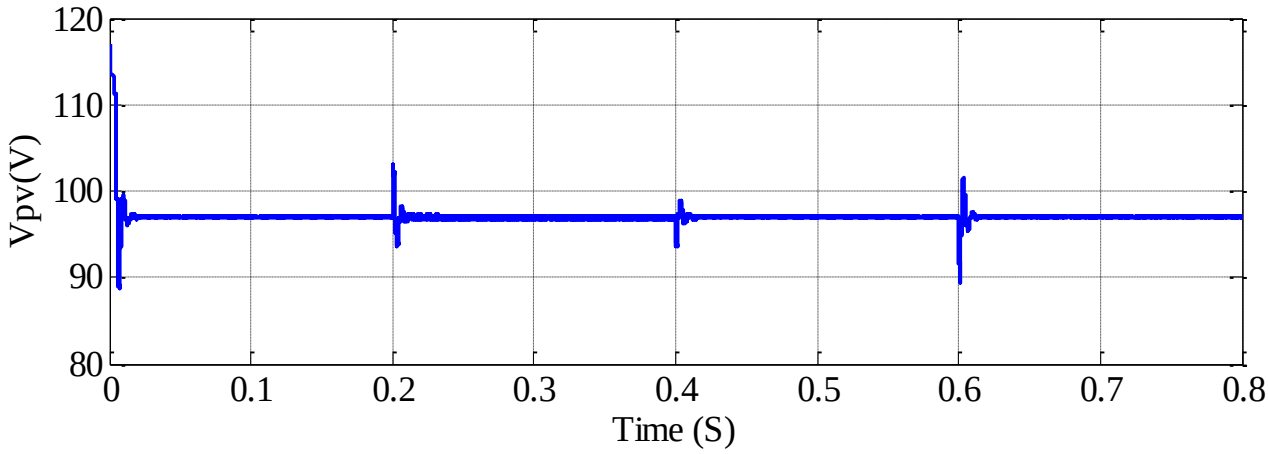

Figure 3-14: Voltage curve at the GPV terminals

Figure (3-14) represents the actual PVG output voltage. The variation is minimal and that is to say that the adjustment is precise, it goes up and down a little bit. When the sense changes the curve makes harmonics, and it means that Vpv and Vpv_{ref} are very close to each other.

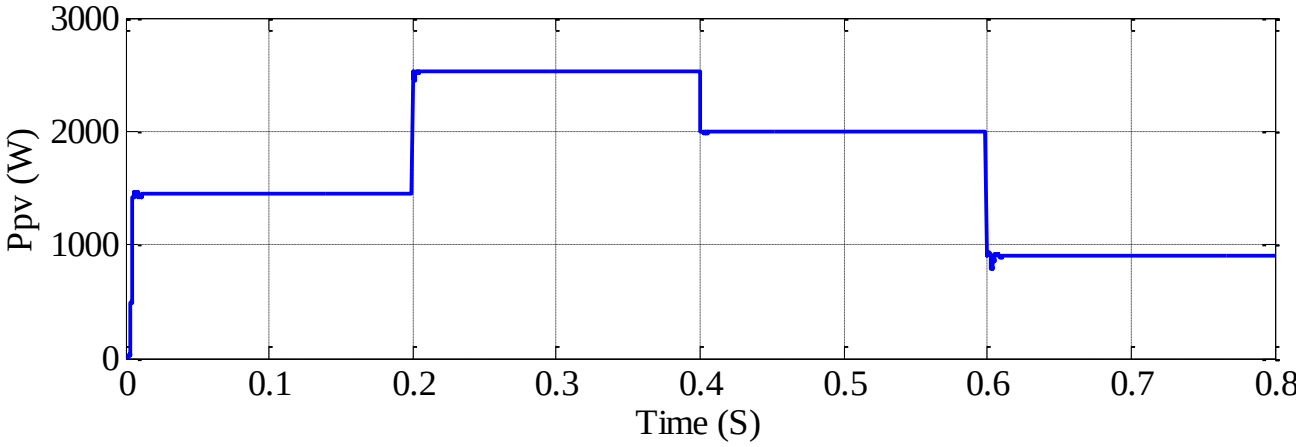

Figure 3-15: Power curves at the GPV terminals

According to the figure (3-15), we notice that the power reacts according to the solar irradiance and this is always fixed at the maximum power.

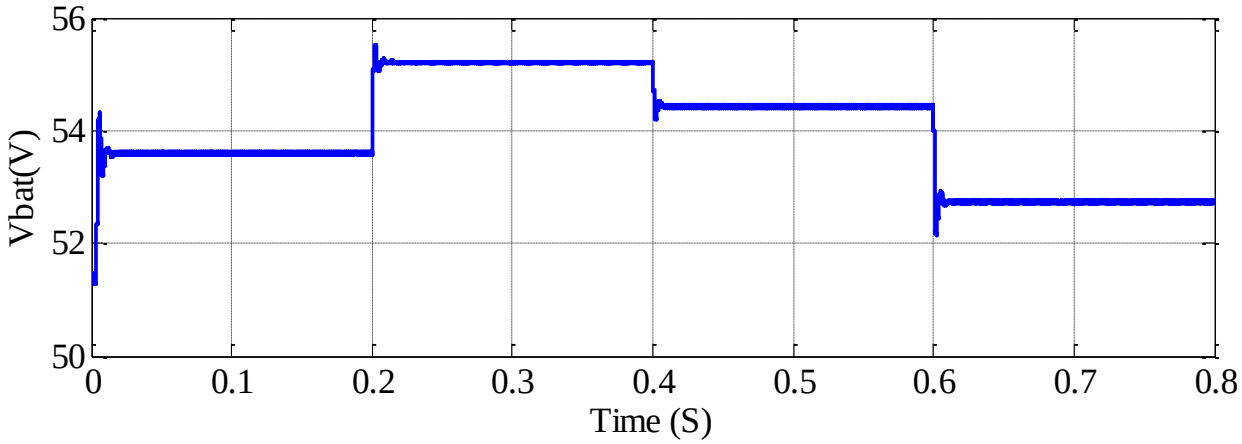

Figure 3-16: Battery voltage curve

In the curve in figure (3-16), we perceive ripples in the curve of the battery voltage so the MPPT works well, i.e., the battery tuning loop is working and it reacts according to the solar irradiance.

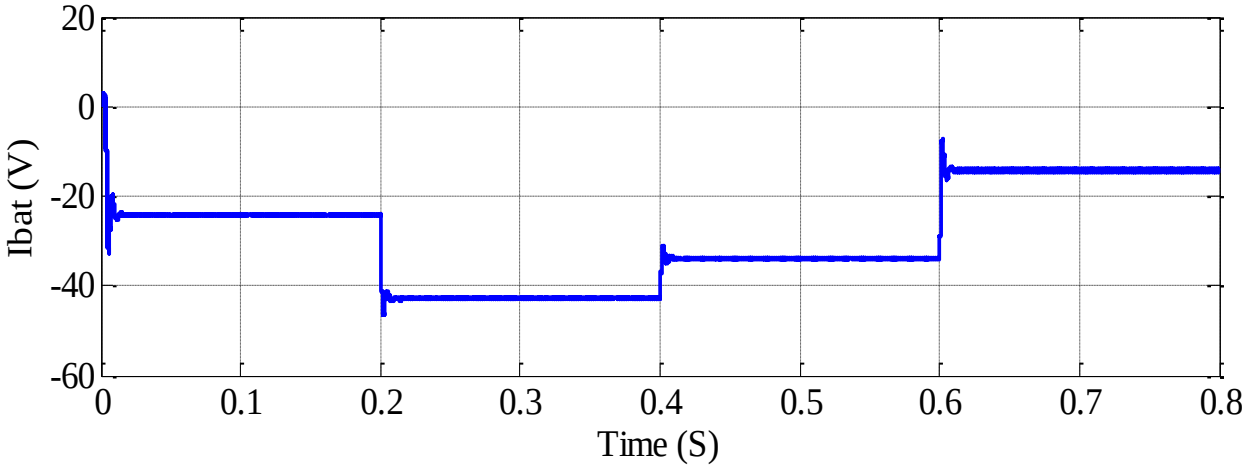

Figure 3-17: Battery current curve

According to the curve obtained in figure (3-17), the load was powered in the beginning, when the solar irradiance is low that's mean that the battery powered the load so the sense is positive and when we have enough solar irradiance the current curve is negative that's to say the battery is being charged. After 0.6 S the battery was charged and it began to powered the system.

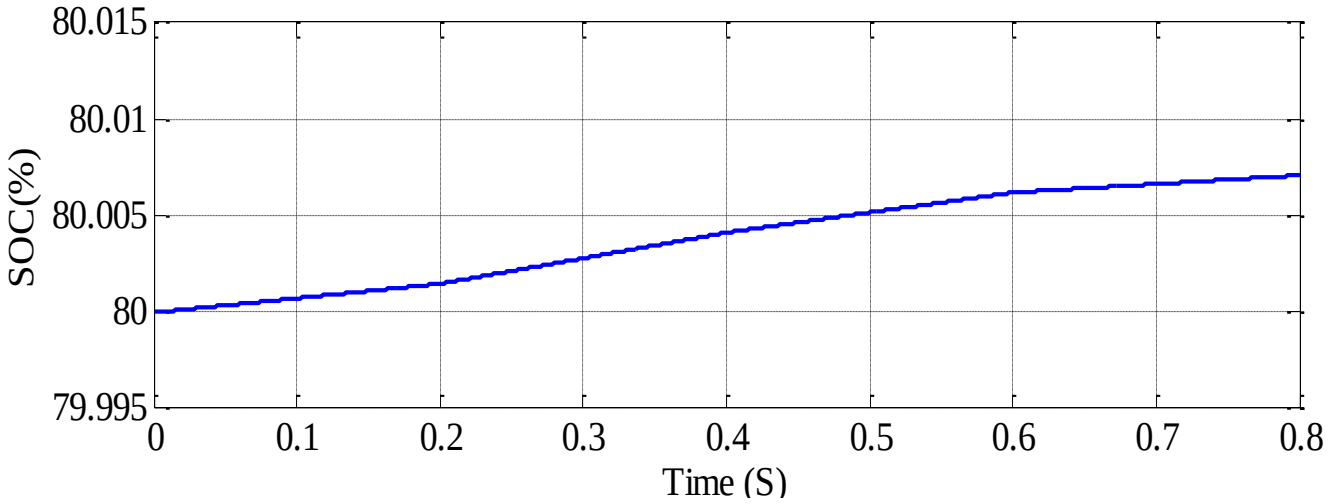

Figure 3-18: Battery state of charge curve

According to the curve obtained in figure (3-18). The initial state of charge is set at 80%, which is a high value and challenging to increase further.

3.12.2 Scenario N° 2: Temperature variation

The temperature is varied according to the figure (3-19); while maintaining the solar irradiance and the load.

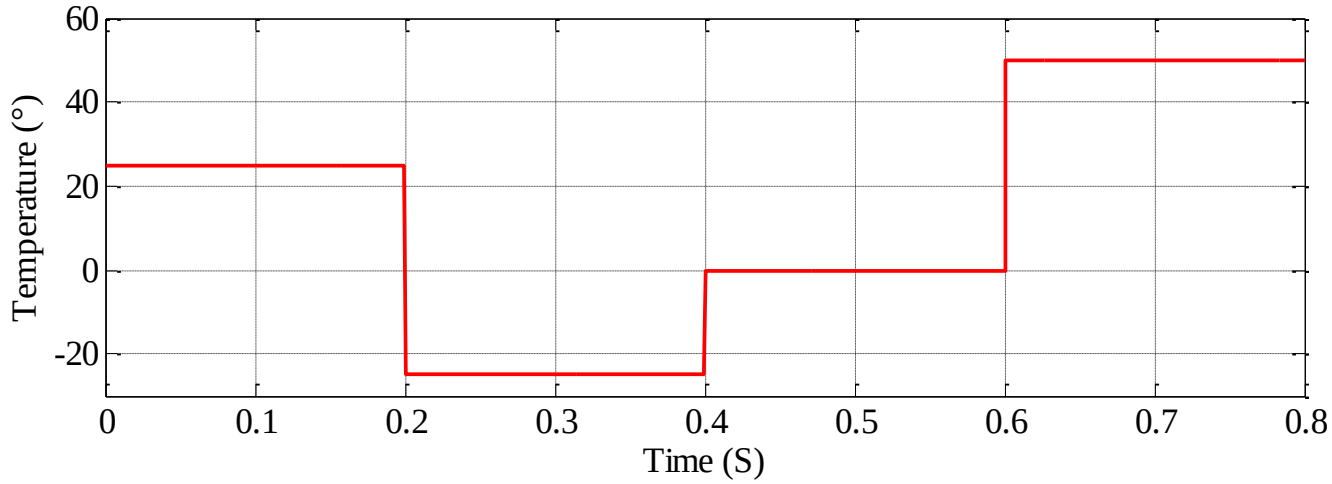

Figure 3-19: Temperature curve

From the given curve in figure (3-19) it can be seen that we changed the temperature from -25° to 50° in a step of 25° in order the see the temperature effect. The temperature influences the rest despite we fixed the solar irradiance and the load.

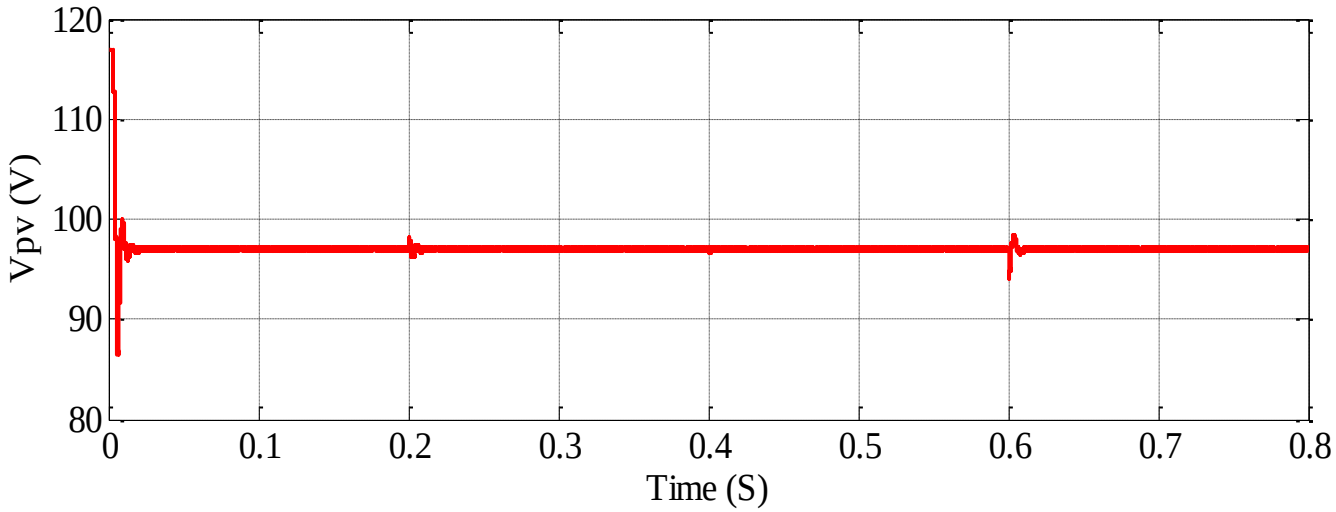

Figure 3-20: Voltage curve at the GPV terminals

Figure (3-20) represents the actual PVG output voltage. The variation is minimal and i.e., that the adjustment is precise, it goes up and down a little bit, the curve in figure 3-20 has harmonics, indicating that Vpv and Vpv_{ref} are in close proximity to each other.

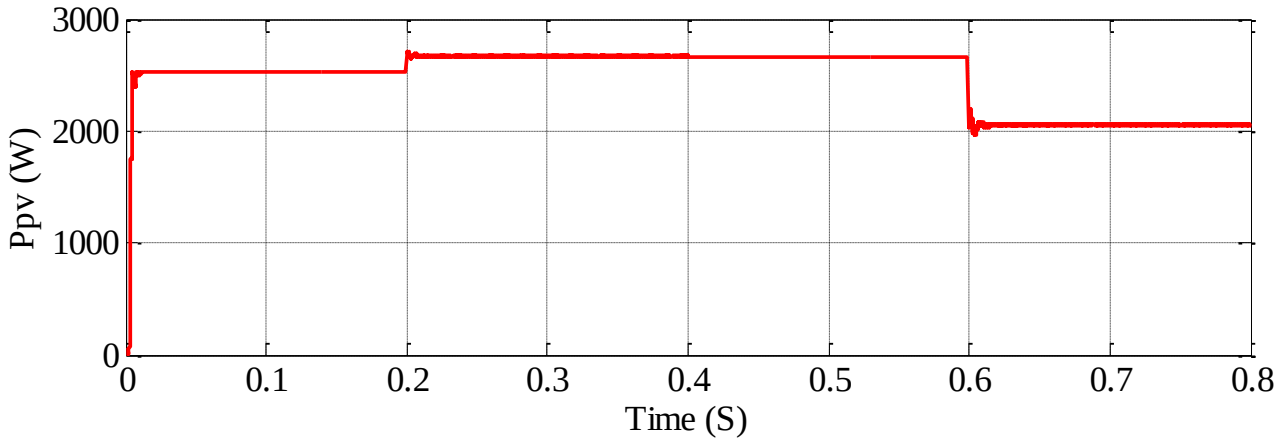

Figure 3-21: Power curve at the GPV terminals

According to the curve obtained in figure (3-21). We noticed that the power at the GPV terminals reacts according to the solar irradiance in each in every stage regardless the temperature. But with somewhat similar values.

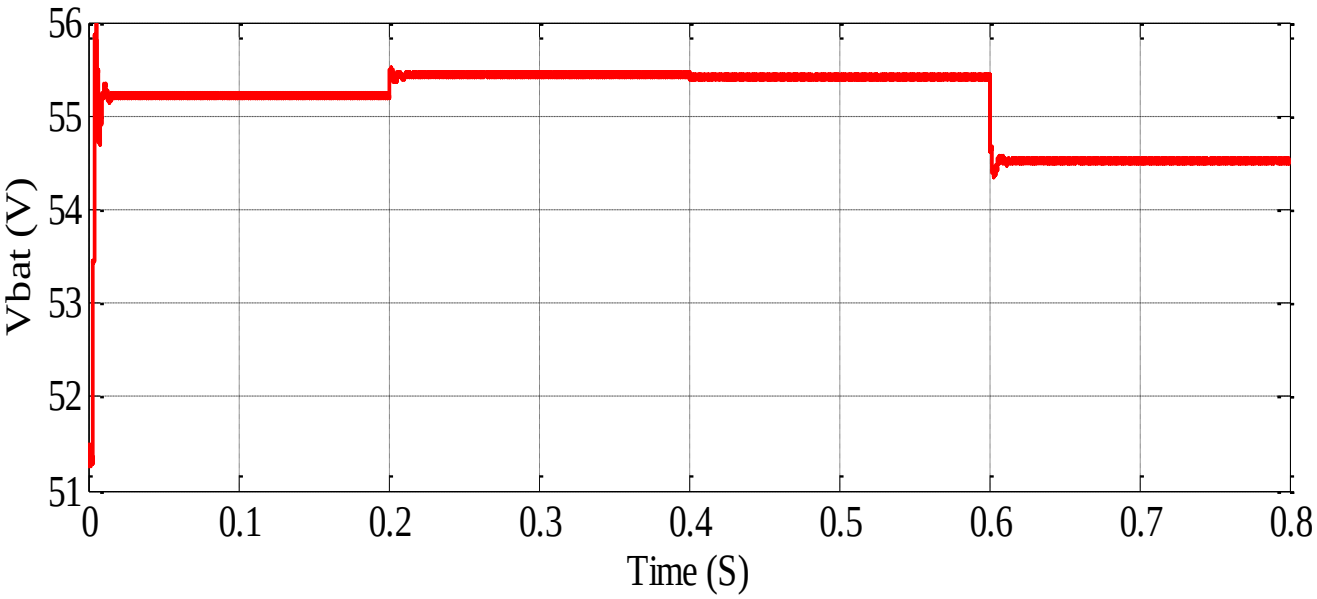

Figure 3-22: Battery voltage curve

In the curve shown in figure (3-22) we can see that the presence of fluctuations in the battery voltage curve indicates the effective operation of the MPPT system. This suggests that the battery tuning loop is functioning correctly and responding appropriately to temperature values.

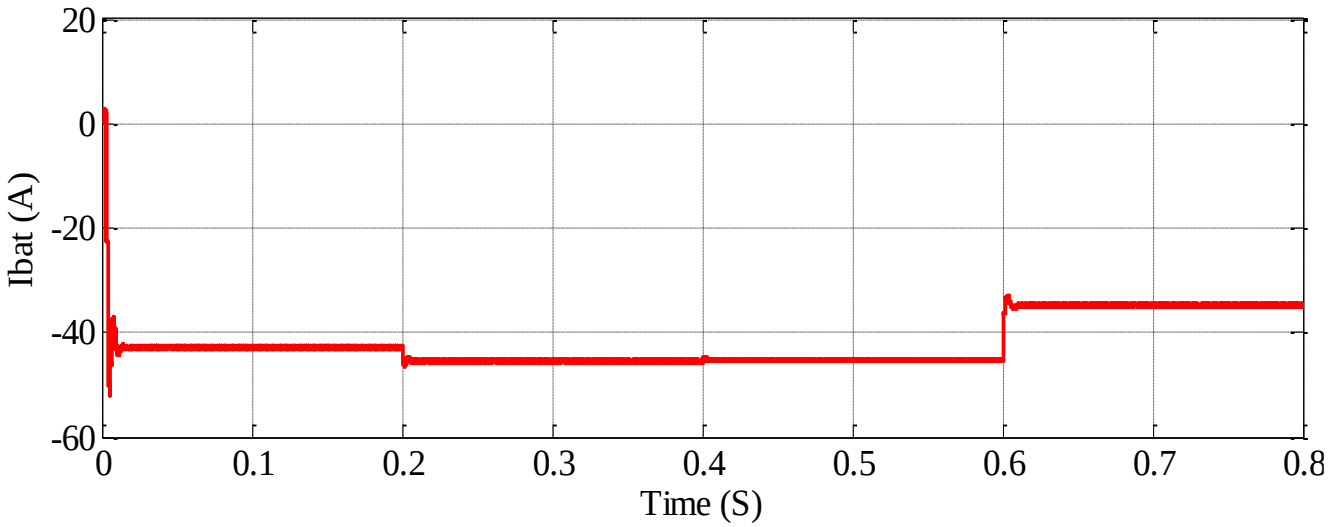

Figure 3-23: Battery current curve

According to the curve obtained in figure (3-23). Initially, when the temperature is low, the load is powered by the battery, resulting in a positive sense in the current curve. As the temperature increases, the current curve becomes negative, indicating that the battery is being charged. After 0.6 seconds, the battery reaches a fully charged state and starts powering. And all this is with little values not like the effect of the solar irradiance variation with constant temperature.

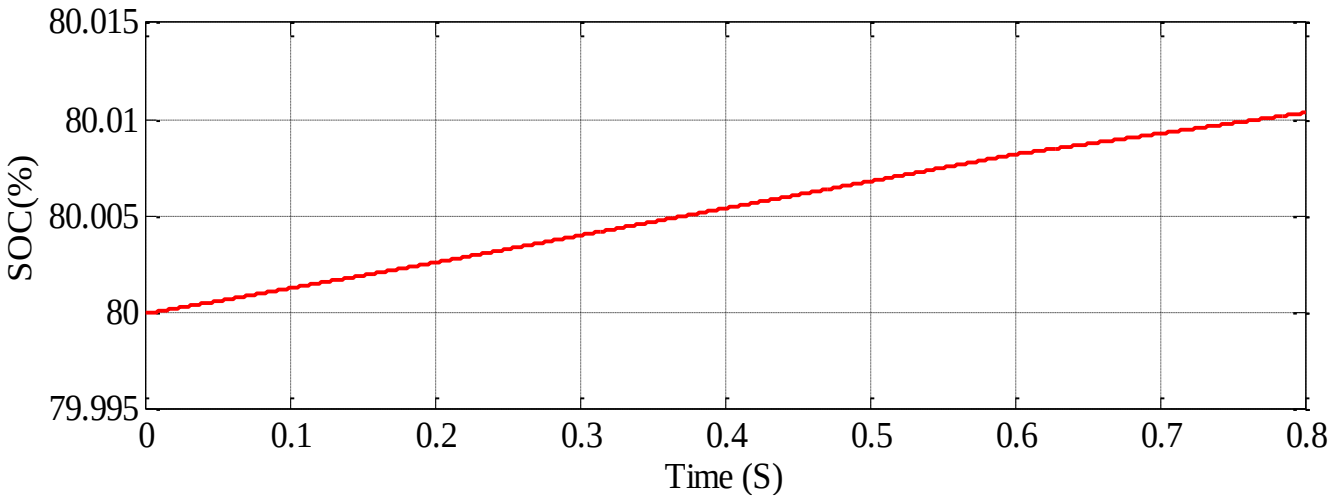

Figure 3-24: Battery state of charge curve

According to the curve obtained in figure (3-24). The initial state of charge is set at 80%, which is a high value and challenging to increase further.

3.12.3 Scenario N° 3: Load variation

We vary the load (load current) according to the figure (3-25); while maintaining the solar irradiance at 800 W/m² and the temperature

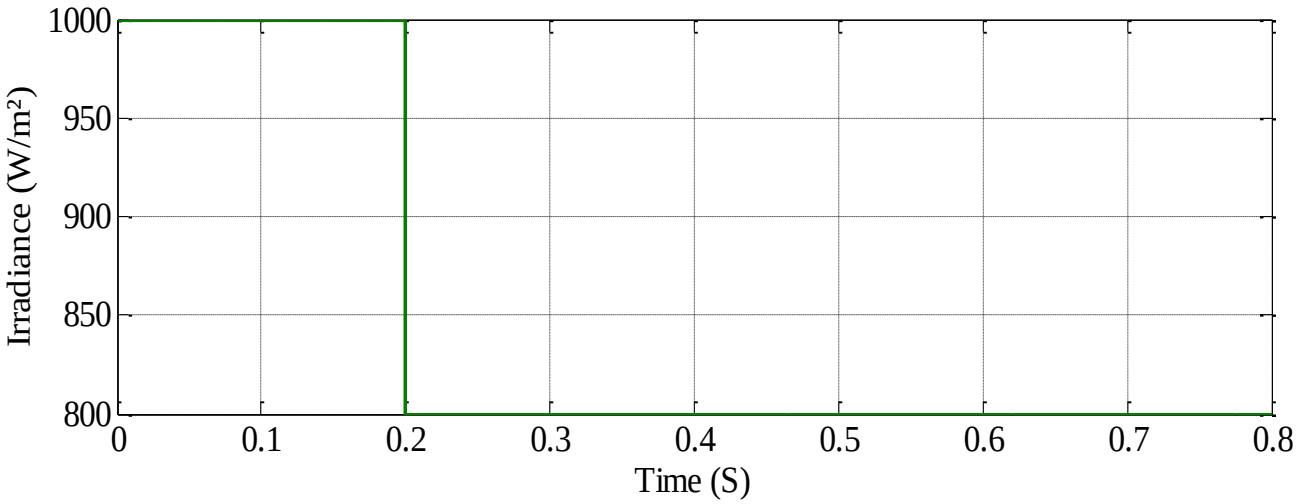

Figure 3-25: Solar irradiance curve

In the curve obtained in figure (3-25) we changed the solar irradiance only once from 1000 (W/m²) to 800 (W/m²), in order to see the effect of the load variation.

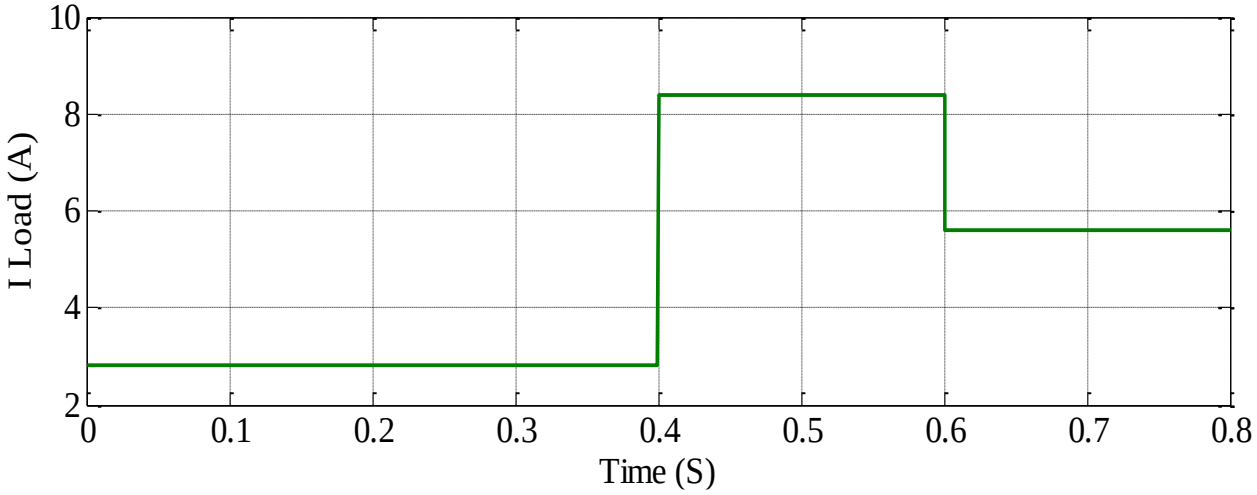

Figure 3-26: Load current curve

From the given curve in figure (3-26). From 0.2 S to 0.8 S, we have the same solar irradiance with the three values of the load current 2.8A,5.6A,8.4A in order to see the load effect.

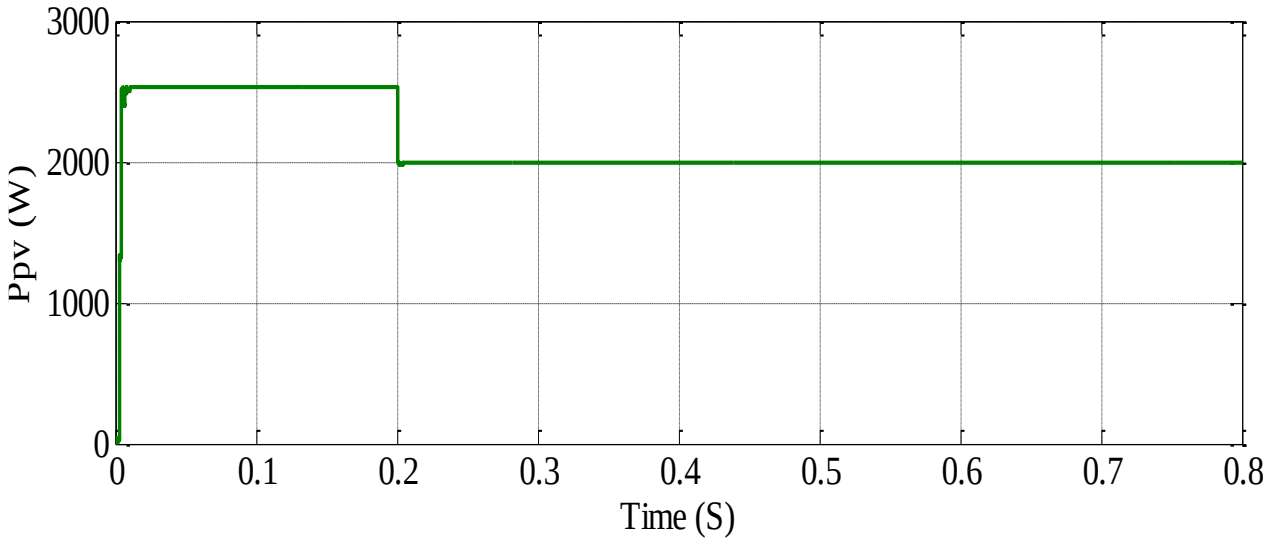

Figure 3-27: Power curve at the GPV terminals

According to the figure (3-27). Regardless of the load value, the power output of the system remains unaffected it reacts according to the solar irradiance. And the system continues to provide energy due to the presence of a battery that charges and supplies power.

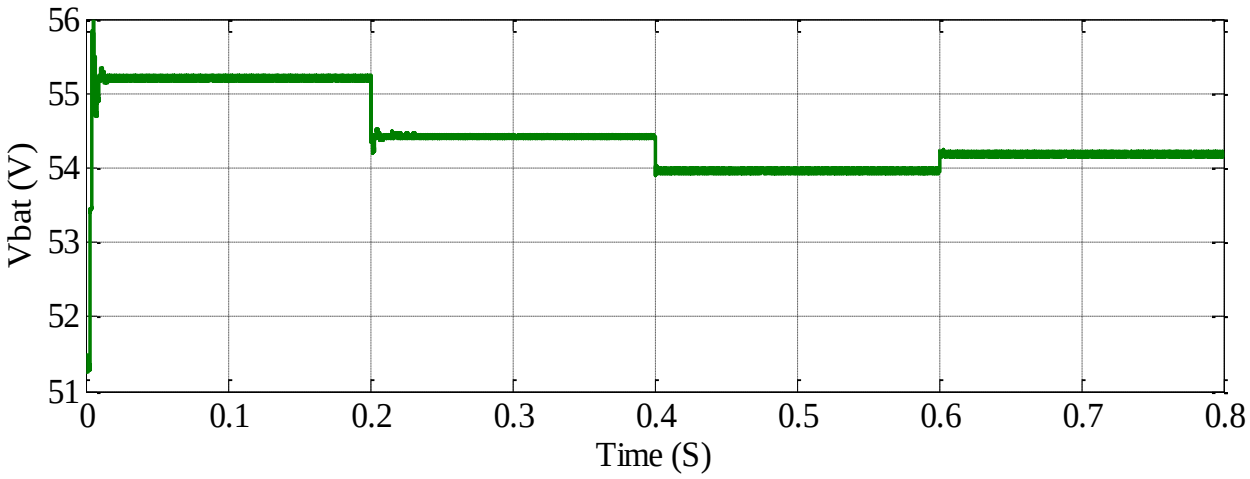

Figure 3-28: Battery voltage curve

From the given curve in figure (3-28). There are ripples in the curve of the battery voltage so the MPPT works well, i.e., the battery tuning loop is working and it reacts according to the load.

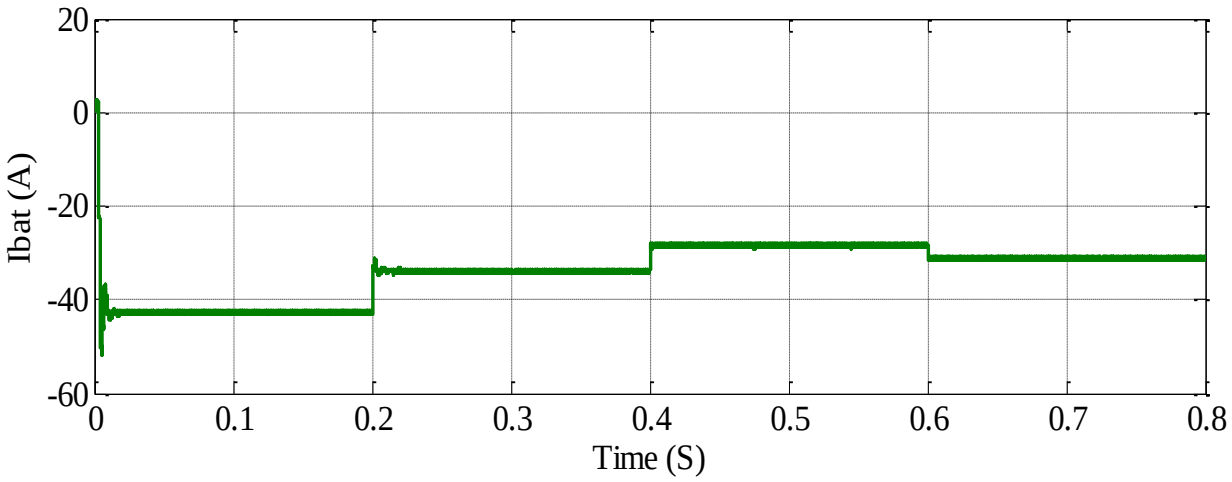

Figure 3-29 : Battery current curve

According to the curve obtained in figure (3-29). The load was powered in the beginning, when the load value is low that's mean that the battery powered the load so the sense is positive and when we have enough load the current curve is negative that's to say the battery is being charged.

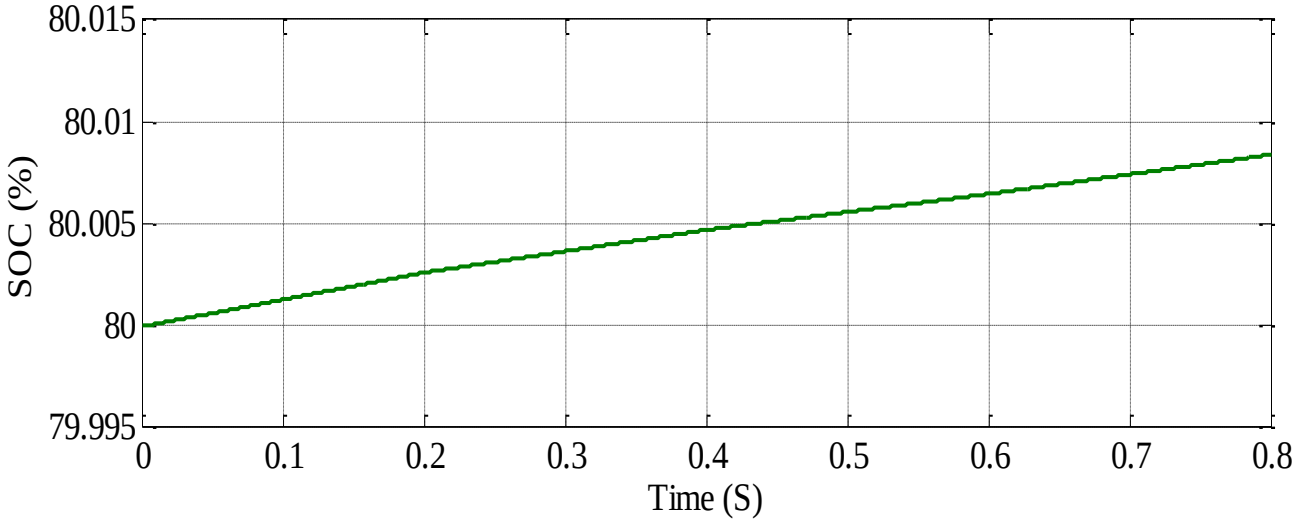

Figure 3-30 : Battery state of charge curve

According to the curve obtained in figure (3-30). The initial state of charge is set at 80%, which is a high value and challenging to increase further.

3.13 Conclusion

The use of a fuzzy controller for MPPT in photovoltaic systems offers significant advantages in terms of efficiency and energy production optimization. This approach allows for the optimal utilization of photovoltaic solar energy, which explains its growing use worldwide.

fuzzy logic control can be seen as a step towards a rapprochement between precise mathematical control and human decision-making and the results confirm the correct operation of the fuzzy controller, it has proven to have better performance, fast response time and very low steady-state error, and is robust to different variations in atmospheric conditions.

GENERAL CONCLUSION

General conclusion

This work was dedicated to a study on the control and optimization of a stand-alone photovoltaic system using fuzzy logic controller. One can quickly understand and justify the interest in photovoltaic solar energy. Firstly, photovoltaic solar energy is a clean, silent, available, and free source of energy. It is precisely this fact that explains its significant growth in utilization worldwide. In order to enhance the efficiency of photovoltaic systems, the fuzzy logic technique was studied for maximum power point tracking (MPPT).

In this work, we conducted a study on the modeling of a photovoltaic system, which consists of a photovoltaic generator, a power conditioning stage (DC/DC Buck converter), a battery loaded on a DC bus voltage, and a control stage to drive the converter using fuzzy MPPT control.

In the first chapter, we provided a general overview of the state of the art in photovoltaic energy and the types of solar energy on one hand, and we highlighted the advantages and disadvantages of photovoltaic energy on the other hand.

In the second chapter, we explained the operating principle of a photovoltaic system. We began with an overview of photovoltaic systems, their functioning principle, and the mathematical model. Subsequently, we presented and analyzed simulation results of photovoltaic panel, considering the effects of temperature and irradiance.

In the full stand-alone PV system studied in the last chapter, a charge controller was designed to integrate both the battery regulation and the fuzzy logic MPPT technique. We conducted multiple simulations and analyses to assess its effectiveness. Following that, we showcased the simulation results of a PV system utilizing the Fuzzy-MPPT controller.

Through this work, we wish to have made a contribution to the study of the photovoltaic characteristics of the solar cell, the study of stand-alone photovoltaic systems and the fuzzy MPPT control.

Bibliographic references

[1] HANANOU, F., & ROUABAH, A. "*Modélisation et simulation d'un système photovoltaïque"*, Master's thesis, Kasdi Merbah University of Ouargla, 2014.

[2] A. R, Jha (2009). "*Solar cell technology and applications*" Book, Taylor and Francis Group, LLC.

[3] https://www.azteksolar.ca/

[4] Maifi, L., & Kerbache, T. (2018). "*Etude et modélisation d'un panneau solaire thermique photovoltaïque* " (Doctoral dissertation, Université Frères Mentouri-Constantine 1).

[5] Dincer, I. (Ed.). (2018). "*Comprehensive energy systems"*. Elsevier.

[6] Created internally by a member of the Energy Education team. Adapted from: Eco green Electrical. (August 14, 2015). Solar PV Systems [Online].

[7] Mr. Solar. (August 13, 2015). "*Photovoltaic Effect*" [Online]. Available, http://www.mrsolar.com/photovoltaic-effect/.

[8] https://www.dosolar.com.au/

[9] Akshay VR "*Solar Irradiance Calculation Guide*", post by Republic of solar, https://thesolarlabs.com/ros/, 2022.

[10] KARKARINE Abdelkader. (2017). "*Modeling and control of a photovoltaic system*". Master thesis, university of Badji Mokhtar-Annaba.

[11] Fethallah, T. A. T. I., & Oussama, B. L. (2018). "*Etude et Réalisation d'un Système Photovoltaïque Optimisé par Logique Floue*". *Mémoire MASTER ACADEMIQUE, UNIVERSITE KASDI MERBAH OUARGLA.*

[12] https://www.perovskite-info.com/

[13] LAMARA, M. (2022). "*Etude comparative des algorithmes P&O et Inc-Cond pour l'optimisation d'un système photovoltaïque (PV) autonome*" (Doctoral dissertation, university of M'sila).

[14] Bouchareb Khalil, T. A. (2021). "*Modélisation et simulation d'un système PV adapté par une commande MPPT basée sur un mode glissant*".

[15] Imed, K., Hafaifa, A., & Abdellah, K. (2016, October). "*Performance analysis of a photovoltaic system based on solar irradiance values to obtain the optimum maximum power point*". In *The 9th International Electrical Engineering Conference CEE* (pp. 2-4).

[16] https://www.arinenergy.com/

[17] Salim, A., & Dalila, T. (2017). "*Etude d'un système photovoltaïque*" (Doctoral dissertation, Université Mouloud Mammeri).

[18] Houari, A. (2012). "*Contribution à l'étude de micro-réseaux autonomes alimentés par des sources photovoltaïques*". Université de Lorraine.

[19] G. N. Tiwari, S. Dubey. (2010). "*Fundamentals of Photovoltaic Modules and Their applications*". Book, Cambridge.

[20] John Wiley & Sons Ltd. (2017). "*Photovoltaic Power System Modeling, Design, and Control*". Book, university of Sydney Australia.

[21] AOUICHAT, F. "*Contrôle et optimisation d'un système photovoltaïque (PV) autonome* ", Master's thesis, University of M'sila)., 2021

[22] Mohan, N., Undeland, T. M., & Robbins, W. P. (2003). "*Power electronics: converters, applications, and design*". John wiley & sons.

[23] Messaoud, M., & Haddi, B. (2021). "*Optimum Parametric Identification of a Stand-Alone Photovoltaic System with Battery Storage and Optimization Controller Using Averaging Approach Optimum Parametric Identification of a Stand-Alone Photovoltaic System with Battery Storage and Optimization Controller Using Averaging Approach*". Journal Européen des Systèmes Automatisés, *54*(1), 63-71.

[24] A. Belkaid, 2015. "*Conception et implémentation d'une commande MPPT de haute performance pour une chaine de conversion photovoltaïque autonome*". Thèse de doctorat, Université de Sétif

[25] "*Photovoltaic Power System Modeling, Design, and Control*" by Weidong Xiao (z-lib.org)

[26] Hajighorbani, S., Radzi, M. M., Ab Kadir, M. Z. A., Shafie, S., Khanaki, R., & Maghami, M. R. (2014). "*Evaluation of fuzzy logic subsets effects on maximum power point tracking for photovoltaic system*". International Journal of Photoenergy.

[27] Hilloowala, R. M., & Sharaf, A. M. (1992, October). "*A rule-based fuzzy logic controller for a PWM inverter in photo-voltaic energy conversion scheme*". In Conference Record of the 1992 IEEE Industry Applications Society Annual Meeting (pp. 762-769). IEEE.

[28] Won, C. Y., Kim, D. H., Kim, S. C., Kim, W. S., & Kim, H. S. (1994, June). "*A new maximum power point tracker of photovoltaic arrays using fuzzy controller*". In Proceedings of 1994 Power Electronics Specialist Conference-PESC'94 (Vol. 1, pp. 396-403). IEEE.

[29] Lei, S. F. (1999). "*Solar peak power point tracking*".

[30] Robles Algarín, C., Taborda Giraldo, J., & Rodriguez Alvarez, O. (2017). "*Fuzzy logic based MPPT controller for a PV system*". *Energies*, *10*(12), 2036.

[31] Hussian, O. S., Elsayed, H. M., & Hassan, M. M. (2019, September). "*Fuzzy logic control for a stand-alone PV system with PI controller for battery charging based on evolutionary technique*". In 2019 10th IEEE International Conference on Intelligent Data Acquisition and Advanced Computing Systems: Technology and Applications (IDAACS) (Vol. 2, pp. 889-894). IEEE.

[32] Patcharaprakiti, N., Premrudeepreechacharn, S., & Sriuthaisiriwong, Y. (2005). "*Maximum power point tracking using adaptive fuzzy logic control for grid-connected photovoltaic system*". Renewable Energy, 30(11), 1771-1788.

[33] Mamdani, E. H., & Assilian, S. (1975). "*An experiment in linguistic synthesis with a fuzzy logic controller*". International journal of man-machine studies, 7(1), 1-13.

[34] Sugeno, M., & Kang, G. T. (1988). "Structure identification of fuzzy model. *Fuzzy sets and systems*", 28(1), 15-33.

[35] Klir, G., & Yuan, B. (1995). "*Fuzzy sets and fuzzy logic*" (Vol. 4, pp. 1-12). New Jersey: Prentice Hall.

[36] Bezdek, J. C. (2013). "*Pattern recognition with fuzzy objective function algorithms*". Springer Science & Business Media.

[37] Abderezak, L., Aissa, B., & Hamza, S. (2015, June). "*Comparative study of three MPPT algorithms for a photovoltaic system control*". In *2015 World Congress on Information Technology and Computer Applications (WCITCA)* (pp. 1-5). IEEE.

Appendix

Appendix

Table A1. Photovoltaic panel settings

Components	Values
Irradiance at standard STC conditions	1000 W⁄m2
Boltzmann constant	K=1.38 × 10-23 J/K
Electron charge	1.6 × 10-19 C
Diode ideality factor A_n	A_n = 1.6
PV cell temperature at STC	298 K
Number of PV cells per PV module	60
PV panel configuration	3 × 3 PV modules
Power of GPV at MPP and STC	280 W / module
Voltage from GPV to MPP and STC	31.67V
GPV current at MPP and STC	8.84A
Open circuit voltage at STC	38.97V
Short circuit current at STC	9.41A

Table A2. DC bus and battery settings

Battery type	NiMH
Battery model	BK-10V10T
Nominal battery voltage	55 V
Band voltage limits	54,45-55,45 V
Rated battery capacity	90 Ah
Rated voltage of DC load	48 V
DC charging acceptable voltage range	42-56 V

Table A3. Polynomial parameters for modeling the BK-10V10T battery module

Components	Ps5	Ps5	Ps5	Ps5	Ps5	Ps5
Ratings	42.2942	-98.3961	88.7769	-40.3893	10.2942	11.4802

ملخص

تقدم هذا الأطروحة للماجستير تصميمًا وتحجيمًا وتحكمًا في نظام طاقة كهروضوئي مستقل مع شحن البطارية. يستخدم وحدة تحكم الشحن في المحول الجانبي للوحدة الكهروضوئية محول خافض بتيار مستمر. يقوم بنقل طاقة الوحدة الكهروضوئية ، والتي يكون نسبة واجب التبديل هي المتغير (PWM) إلى البطارية وتوفير الطاقة للحمل. باستخدام تقنية تعديل عرض النبضات الذي يتحكم فيه النظام، يتم التحكم بدائرة تكييف الطاقة في الوحدة الكهروضوئية بشكل دائم باستخدام خوارزمية تتبع نقطة القدرة لتحقيق أقصى كمية من الطاقة. يتم الحفاظ على جهد حزمة البطارية بشكل صحيح بواسطة (MPPT) القصوى بمنطق غامض وحدة التحكم في الشحن ويتم تحديده بحيث يتطابق مع تصنيف جهد الحمل، من أجل تجنب الفائض في جهد النظام الكهربائي.

الكلمات المفتاحية :شحن البطارية، التوسيط في مجال الحالة، تخطيط خطي، نموذج صغير للإشارة، وحدة تحكم.

Résumé

Ce mémoire de master présente la conception, le dimensionnement et le contrôle d'un système d'alimentation photovoltaïque (PV) autonome avec charge de batterie. Le régulateur de charge utilisé dans le convertisseur côté PV (PVSC) est un hacheur abaisseur de tension CC/CC. Il transfère la puissance PV vers la batterie et alimente la charge. En utilisant la technique de modulation de largeur d'impulsion (PWM), dont le rapport cyclique de commutation est la variable de contrôle d'entrée, le circuit de conditionnement de puissance PVSC est constamment contrôlé par un algorithme flou de suivi du point de puissance maximum (MPPT) pour atteindre la puissance maximale. La tension du pack de batteries est correctement maintenue par le régulateur de charge et spécifiée pour correspondre à la tension nominale de la charge, afin d'éviter la surtension dans le système d'alimentation.

Mots-clés : *Recharge de batterie, moyennage dans l''espace d'états, linéarisation, modèle à petit signal, régulateur PID.*

Abstract

This Master's thesis introduces the design, dimensioning, and control of a standalone photovoltaic (PV) power system with battery charging. The charge controller used in the PV-side converter (PVSC) is a DC/DC buck converter. It transfers the PV power to the battery and supplies the load. Using pulse width modulation (PWM) technique, of which the switching duty cycle is the control-input variable; the PVSC power-conditioning circuit is permanently controlled by fuzzy logic maximum power point tracking (MPPT) algorithm to achieve the maximum energy. The battery pack voltage is properly maintained by the charge controller and specified to match the load voltage rating, in order to avoid overvoltage in the power system.

Keywords: *Battery charging, state-space averaging, Linearization, small-signal model, PID controller.*